TECHNICAL REPORT RL-80-2

OPTIMIZING A REAL TIME ACOUSTICAL HOLOGRAPHY SYSTEM

W.F. Swinson
Auburn University

For

Ground Equipment and Missile Structures Directorate
US Army Missile Laboratory

1 October 1979

U.S. ARMY MISSILE COMMAND
Redstone Arsenal, Alabama 35809

DISPOSITION INSTRUCTIONS

DESTROY THIS REPORT WHEN IT IS NO LONGER NEEDED. DO NOT RETURN IT TO THE ORIGINATOR.

DISCLAIMER

THE FINDINGS IN THIS REPORT ARE NOT TO BE CONSTRUED AS AN OFFICIAL DEPARTMENT OF THE ARMY POSITION UNLESS SO DESIGNATED BY OTHER AUTHORIZED DOCUMENTS.

TRADE NAMES

USE OF TRADE NAMES OR MANUFACTURERS IN THIS REPORT DOES NOT CONSTITUTE AN OFFICIAL ENDORSEMENT OR APPROVAL OF THE USE OF SUCH COMMERCIAL HARDWARE OR SOFTWARE.

UNCLASSIFIED

SECURITY CLASSIFICATION OF THIS PAGE *(When Data Entered)*

REPORT DOCUMENTATION PAGE		READ INSTRUCTIONS BEFORE COMPLETING FORM
1. REPORT NUMBER RL-80-2	2. GOVT ACCESSION NO.	3. RECIPIENT'S CATALOG NUMBER
4. TITLE *(and Subtitle)* OPTIMIZING A REAL TIME ACOUSTICAL HOLOGRAPHY SYSTEM		5. TYPE OF REPORT & PERIOD COVERED Technical Report 6. PERFORMING ORG. REPORT NUMBER
7. AUTHOR(s) Dr. W. F. Swinson , Auburn University		8. CONTRACT OR GRANT NUMBER(s) DA1L162303A214
9. PERFORMING ORGANIZATION NAME AND ADDRESS Commander US Army Missile Command ATTN: DRSMI-RL Redstone Arsenal, Alabama 35809		10. PROGRAM ELEMENT, PROJECT, TASK AREA & WORK UNIT NUMBERS AMCMS 6123032140911
11. CONTROLLING OFFICE NAME AND ADDRESS Commander US Army Missile Command ATTN: DRSMI-RPT Redstone Arsenal, Alabama 35809		12. REPORT DATE 1 October 1979 13. NUMBER OF PAGES 52
14. MONITORING AGENCY NAME & ADDRESS *(if different from Controlling Office)*		15. SECURITY CLASS. *(of this report)* Unclassified 15a. DECLASSIFICATION/DOWNGRADING SCHEDULE

16. DISTRIBUTION STATEMENT *(of this Report)*

Approved for public release; distribution unlimited.

17. DISTRIBUTION STATEMENT *(of the abstract entered in Block 20, if different from Report)*

18. SUPPLEMENTARY NOTES

This work was accomplished through the Laboratory Research Cooperative Program (LRCP) between Dr. W.F. Swinson of the Department of Mechanical Engineering, Auburn University, and the US Army Missile Command.

19. KEY WORDS *(Continue on reverse side if necessary and identify by block number)*

Acoustical Holography
Real time
Flaw Detection and Quantification
Laser and Optical Reconstruction
Resolution

20. ABSTRACT *(Continue on reverse side if necessary and identify by block number)*

This report documents work performed to improve a real time acoustical holography system used for the detection of flaws and disbonds in structures. The wave propagation phenomena and acoustical imaging techniques are discussed. A series of experiments were conducted to find optimum system alignment for improving image resolution. Sample real time acoustical holograms of flawed specimens are included in the work. A list of suggested system improvements is also given.

DD FORM 1 JAN 73 1473 EDITION OF 1 NOV 65 IS OBSOLETE

UNCLASSIFIED

SECURITY CLASSIFICATION OF THIS PAGE *(When Data Entered)*

CONTENTS

I. Introduction and Theory 5

A. Acoustical Waves 5

B. Wave Propagation 8

II. Experimental Configuration and Observations . . 15

A. Observations 15

B. Rearrangement of System 15

C. Turning the System On 17

D. Acoustical Alignment Techniques 24

E. Comments on Components in the System 27

F. Examples 34

III. Conclusions and Recommendations 42

ILLUSTRATIONS

Figure		Page
1.	Division of an Impinging Acoustical Beam	6
2.	Wave Propagation	9
3.	Acoustical Holography Layout	16
4.	Arthir Rearrangement	18
5.	System Isolation	18
6.	Acoustical Liquid Lens	19
7.	Reference Transducer and Reflector	19
8.	Object Support	20
9.	Optics	20
10.	Electronic Controls	21
11.	Timing and Monitor Controls	21
12.	Capacitors	22
13.	Power Supply and Controls	22
14.	Oscillator Controls	23
15.	TV Set-Up	23
16.	Object Beam Ripple	26
17.	Reference Beam Ripple	26
18.	5 MHz Image	28
19.	3 MHz Image	28
20.	3 MHz, without Minitank, Image	28

ILLUSTRATIONS (Concluded)

Figure		Page
21.	Nearfield Pressure versus Axial Distance	29
22.	Nearfield Pressure Distribution	30
23.	Compound Lens System	32
24.	Plexiglass Sample With An Opaque Mask	35
25.	Acoustical Hologram of the Plexiglas Sample With An Opaque Mask	35
26.	Silica Impacted Model	36
27.	Impacted Model Hologram	36
28.	Steel-Silica Model with Flaws	38
29.	Circular Flaw Hologram	38
30.	Rectangular Flaw Hologram	39
31.	Flaw Hologram with CW Lens	39
32.	Tapered Silica Cracked Model	40
33.	Crack Hologram	40
34.	Cracks and Interference Bars	41
35.	Silica-Epoxy Internal Cracked Model	41
36.	Internal Cracked Model Hologram	42
37.	Epoxy-Glass Cylinder	43
38.	Circular Flaw Hologram of Cylinder	43
39.	Plaster Window	44

I. Introduction and Theory

The purpose of this report is to document ways to enhance the image qualities of an acoustical real time holographic image reproduction system (ARTHIR) developed by Ireland, Mullinix and Castle for the Ground Equipment and Missile Structures Directorate, Technology Laboratory, US Army Missile Research and Development Command, Redstone Arsenal, Alabama (Technical Report T-78-10, October 1977).

The components of the system are well designed and function reliably; however, some changes are suggested that enhance the image quality of ARTHIR.

To use this system effectively, an operator has to spend time understanding the function of the components. ARTHIR's results are best interpreted with an experienced eye. A brief write-up of acoustical wave behavior is included in the following section to help an operator in understanding ARTHIR's components.

A. Acoustical Waves

Basically there are two types of waves in acoustical sonic transmission: transverse waves and longitudinal waves. Transverse waves (called shear waves) vibrate transverse or perpendicular to the direction of the propagating wave. An analogy of this type of vibration is seen when a rock is dropped in a pool of water. Waves propagate outward at the same time a cork floating on the water surface is seen to bob (vibrate) up and down indicating that the vibration is perpendicular (transverse) to the direction of wave propagation. Light is an example of transverse waves as evidenced by polarization. A longitudinal wave is a wave that vibrates in the same direction as the wave propagation. An analogy of this might be visualized by imagining a train whose cars are connected by springs. As the engine starts up it takes time for the last car to sense the motion induced by the engine, and when it does, it sends a motion back to the engine. Without friction this oscillation would continue in a longitudinal vibration.

When an acoustical wave (say a longitudinal wave) in one medium intersects the surface of another medium several things in general happen (Figure 1). The impinging (assumed plane wave) wave divides up into several waves (Figure 1):

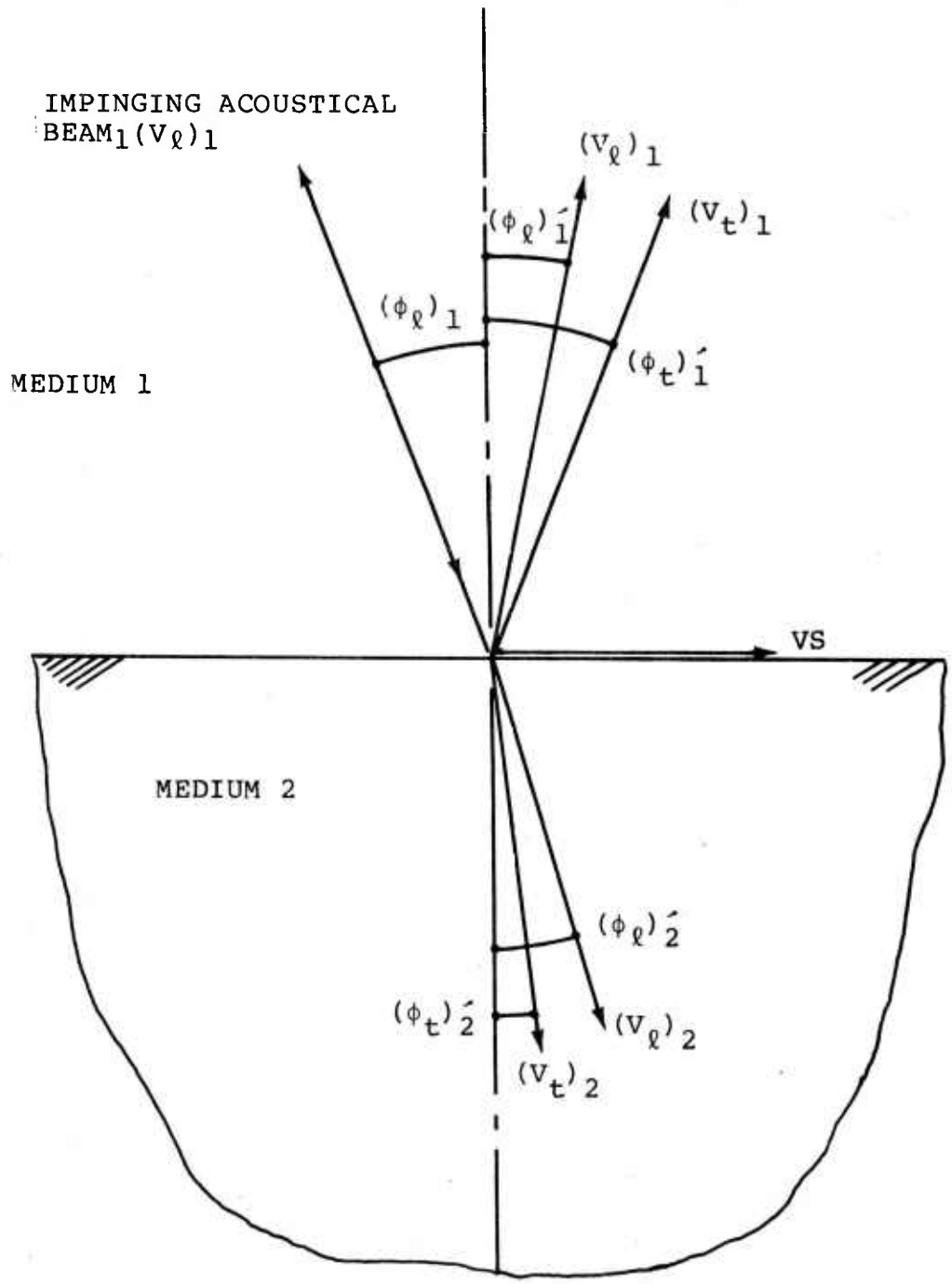

Figure 1. Division of an impinging acoustical beam.

- A reflected transverse wave with wave front velocity $(v_t)_1$ at an angle $(\phi_t)'_1$;
- A reflected longitudinal wave with wave front velocity $(v_\ell)_1$ at an angle $(\phi_\ell)'_1$;
- A refracted transverse wave with wave front velocity $(v_t)_2$ at an angle $(\phi_t)'_2$;
- A refracted longitudinal wave with wave front velocity $(v_\ell)_2$ at an angle $(\phi_\ell)'_2$; and possibly
- A surface wave (called a Rayliegh wave) traveling at a velocity (v_s) along the interface of the two mediums.

Snell's law is used to predict angles of refraction and reflection.

$$\frac{\sin(\phi_\ell)_1}{(v_\ell)_1} = \frac{\sin(\phi_\ell)'_1}{(v_\ell)_1} = \frac{\sin(\phi_t)'_1}{(v_t)_1} = \frac{\sin(\phi_\ell)'_2}{(v_\ell)_2} = \frac{\sin(\phi_t)'_2}{(v_t)_2} \tag{1}$$

It can be surmised from equation [1] that as $(\phi_\ell)_1$ increases so does $(\phi_\ell)'_2$ and at some angle, called the first critical angle, $(v_\ell)_2$ is along the interface. As $(\phi_\ell)_1$ is increased further no longitudinal wave is refracted and a second critical angle is formed such that $(v_t)_2$ is along the interface. These angles are sensitive and important in various testing procedures. Also note that if the impinging longitudinal plane wave is normal to the second medium no transverse waves are produced.

To give some background in propagation velocities, consider the differential equations of equilibrium for solids in terms of displacements with the inertial terms added

$$\begin{aligned}
(\lambda + G)\ \frac{\partial e}{\partial x} + G\nabla^2 u - \rho\ \frac{\partial^2 u}{\partial t^2} &= 0 \\
(\lambda + G)\ \frac{\partial e}{\partial y} + G\nabla^2 v - \rho\ \frac{\partial^2 v}{\partial t^2} &= 0 \\
(\lambda + G)\ \frac{\partial e}{\partial z} + G\nabla^2 w - \rho\ \frac{\partial^2 w}{\partial t^2} &= 0
\end{aligned} \tag{2}$$

where

λ, G = Lame's constants

e = volume expansion = $\varepsilon_x + \varepsilon_y + \varepsilon_z$ (sum of normal strain components)

u, v, w = displacements in the x, y, and z directions, respectively

ρ = density of material

$\frac{\partial^2 u}{\partial t^2}, \frac{\partial^2 v}{\partial t^2}, \frac{\partial^2 w}{\partial t^2}$ = accelerations in x, y, z directions of a point in vibration

$\nabla^2 = \frac{\partial^2}{\partial x^2} + \frac{\partial^2}{\partial y^2} + \frac{\partial^2}{\partial z^2}$, an operator

Theoretical waves of distortion (transverse waves) are modeled by assuming that the volume expansion is zero, e = 0, then equations [2] reduce to

$$G\nabla^2 u - \rho \frac{\partial^2 u}{\partial t^2} = 0$$

$$G\nabla^2 v - \rho \frac{\partial^2 v}{\partial t^2} = 0 \qquad (3)$$

$$G\nabla^2 w - \rho \frac{\partial^2 w}{\partial t^2} = 0$$

B. Wave Projection

Now further restrict the acoustic vibration such that the x-axis is the assumed direction of propagation and the y-axis is the transverse particle vibration direction.

Thus, u = w = 0 and equations [3] become

$$\frac{\partial^2 v}{\partial t^2} = \sqrt{\frac{G}{\rho}} \quad \frac{\partial^2 v}{\partial x^2} \qquad (4)$$

A general form of the solution of this equation is

$$v = f(x + \sqrt{\frac{G}{\rho}}\ t) + f_1\ (x - \sqrt{\frac{G}{\rho}}\ t) \qquad (5)$$

where f and f_1 can be any function. To interpret the meaning of this solution consider f_1 and its argument, $(x - \sqrt{G/\rho}\ t)$. Assume f_1 is of the form, (abc) illustrated in Figure 2 for a given time, t.

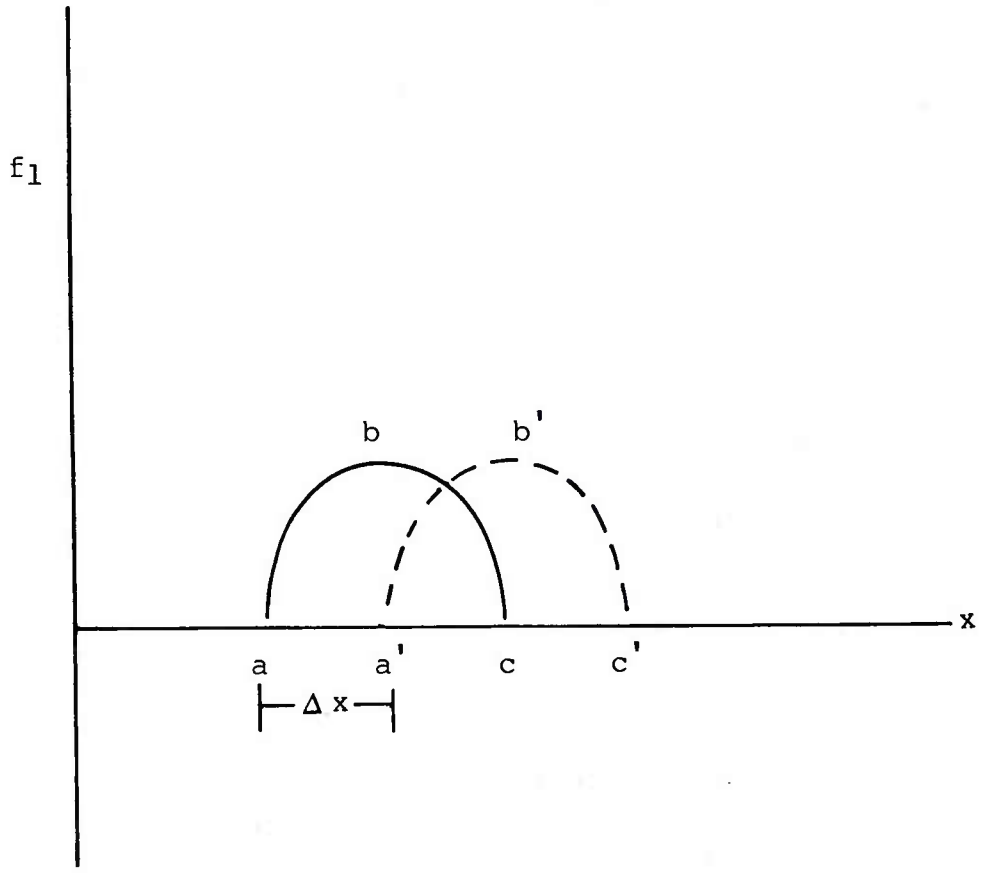

Figure 2. Wave Propagation.

At a later time, say $t + \Delta t$, the argument becomes $x - \sqrt{G/\rho}\ (t + \Delta t)$. Observing this argument it can be noted that the argument remains unchanged provided x is increased by Δx equal to $\sqrt{G/\rho}\ \Delta t$. Therefore, the curve abc at time Δt can be used to describe the wave at $t + \Delta t$ (a'b'c') provided it is displaced by Δx. Further interpretation suggests a wave propagation velocity of $\Delta x/\Delta t = \sqrt{G/\rho}$

or $v_t = \sqrt{G/\rho}$ (6)

Theoretical longitudinal waves (irrotational waves or dilitational waves) can be developed from equation [2] by assuming the rotational terms are zero

$$w_z = \frac{1}{2}\left(\frac{\partial v}{\partial x} - \frac{\partial u}{\partial y}\right) = 0$$

$$w_x = \frac{1}{2}\left(\frac{\partial w}{\partial y} - \frac{\partial v}{\partial z}\right) = 0$$

$$w_y = \frac{1}{2}\left(\frac{\partial u}{\partial z} - \frac{\partial w}{\partial x}\right) = 0 \qquad (7)$$

Equations [7] are satisfied if a function ϕ is defined such that

$$u = \frac{\partial \phi}{\partial x}$$

$$v = \frac{\partial \phi}{\partial y} \quad \text{and}$$

$$w = \frac{\partial \phi}{\partial z} \qquad (8)$$

then $e = \nabla^2 \phi$

and $\frac{\partial e}{\partial x} = \nabla^2 u, \quad \frac{\partial e}{\partial y} = \nabla^2 v, \quad \frac{\partial e}{\partial z} = \nabla^2 w$

Substituting these expressions into equation [2] result in

$$(\lambda + 2G)\ \nabla^2 u - \rho \frac{\partial^2 u}{\partial t^2} = 0$$

$$(\lambda + 2G)\ \nabla^2 v - \rho \frac{\partial^2 v}{\partial t^2} = 0$$

$$(\lambda + 2G)\ \nabla^2 w - \rho \frac{\partial^2 w}{\partial t^2} = 0 \qquad (9)$$

Equations [9] are longitudinal waves and by a similar argument as for shear (tranverse waves) the velocity of propagation is

$$v_\ell = \sqrt{\frac{\lambda + 2G}{\rho}} \qquad (10)$$

Similar results for liquids and air exist. For these materials idealized as having no shear stress and for a plane wave the equations of motion reduce to

$$- \frac{\partial p}{\partial x} = \rho \frac{\partial^2 u}{\partial t^2} \quad . \tag{11}$$

For these materials pressure can be related to displacement through the bulk modulus

$$BM = -Vol \frac{\partial p}{\partial Vol} \tag{12}$$

where Vol is volume.

For a plane disturbance (one dimensional wave) equation [12] reduces to

$$\partial p = - (BM) \frac{\partial Vol}{Vol} = - BM \, \partial \frac{\partial u}{\partial x} \tag{13}$$

or

$$\frac{\partial p}{\partial x} = - BM \frac{\partial^2 u}{\partial x^2} \tag{14}$$

Substituting equation [14] into equation [11] results in

$$(BM) \frac{\partial^2 u}{\partial X^2} = \rho \frac{\partial^2 u}{\partial t^2} \tag{15}$$

where the acoustical wave is longitudinal and has a propagation velocity of

$$v_\ell = \sqrt{\frac{BM}{\rho}} \tag{16}$$

This is idealized as isentropic. Table 1 gives some calculated values for acoustical velocities.

Acoustical waves which are excited by sinusoidal inputs have wave lengths dependent on the material (actually velocity of propagation) and the frequency of the input,

$$v = f\lambda \tag{17}$$

where v = velocity of propagation
f = frequency of disturbing (sonic) input
λ = wave length

An important property in transmitting acoustical waves is the reflectance of a wave in one material impinging on the boundary of another material. If the materials are different as for example air and steel most of the wave is reflected. Obviously if the materials were the same then all of the wave would be transmitted. A term used to estimate the amount of reflectance (or transmittance which ever is desired) is acoustical impedance at normal incidence defined as

$$z = \rho v_{\ell} \tag{18}$$

for longitudinal waves. It is noted that when a longitudinal wave in one material intersects a second material at normal incidence then the reflectance is calculated from

$$R = \left[(z_2 - z_1)/(z_2 + z_1)\right]^2 \tag{19}$$

Affecting, significantly, all waves is attenuation of the wave, a property that does not appear in the mathematical formulations. In liquids there are shear stresses which were assumed negligible for a mathematical description. In all materials there is scattering of the waves due to grain size or particles within the material. Some materials will be noted as acoustical absorbers while others will transmit the acoustical waves very well; still other materials are good reflectors.

There is a mathematical description of liquid surface real time acoustical holography, Hildebrand, B.P. and Brenden, B.B., "Introduction to Acoustical Holography", New York: Plenum Press, 1972. Other descriptions available seem to parallel this account.

TABLE 1. Acoustical Properties (Values Calculated from Reference Data)

MATERIAL	MODULUS OF ELASTICITY, E	VELOCITY OF SOUND, v_t ft/sec	IMPEDANCE $z = \rho v_\ell$ lbm/sec in
SOLID:			
STEEL	3(	10469	65938
ALUMINUM	10.(	10360	24416
BRASS	15.(	6896	52986
MAGNESIUM	6.	9878	16457
MONEL	2(	8939	74883
TITANIUM	1	9228	36017
INVAR	2	8628	56180
LIQUID:			
WATER			2107
ALCOHOL			1303
GLYCERIN			3445
MERCURY			28024
LINSEED OIL			1974
GAS:			
AIR			.58

II. Experimental Configuration and Observations

A. Observations

Acoustical waves coming through a model will be "scattered" at the surfaces as well as internally. Intuitively, the sooner (distance wise) the waves can be collected and focused the better. There will be less attenuation in the waves and wave fronts affected by model defects will have more distortion closer to the defect than farther away. Therefore, better holograms are expected with shorter path lengths.

Some models will not be suitable for this type of acoustical inspection. For example a solid steel cylinder with its axis perpendicular to the direction of object wave propagation will act as a diverging lens such that in some cases the acoustical lens cannot collect and focus the waves on the liquid surface. This does not exclude hollow cylinders, nor some solid cylinders with large radii.

Some materials are very good acoustical absorbers and therefore for models made from these materials acoustical holographic results are not expected. Epoxy is an example of a good acoustical absorber, therefore only thin epoxy models can be effectively used. Flaws are usually good absorbers and thus air bubbles, separation between surfaces, cracks and other such flaws should be detectable. All of this of course depends on resolution of the system.

Experience has suggested to this investigator that one to one magnification in interferometry is preferred, and allow well developed film enlargers to magnify the results as needed. Also it is noted that one acoustical lens is preferred over two lenses. One lens is more convenient to align. One lens also gives less distortion of the waves. More will be said about lenses later in this report.

When using large transducers considerable power is needed to insonify the object and represents a problem. If enough power is not available to adequately insonify an object then results will be limited.

B. Rearrangement of System

The acoustical system was rearranged (apparently back to the original configuration), Figures 3 and 4. It was suspected and verified that shorter path lengths reduced attenuation, unwanted scatter and provided more intensity

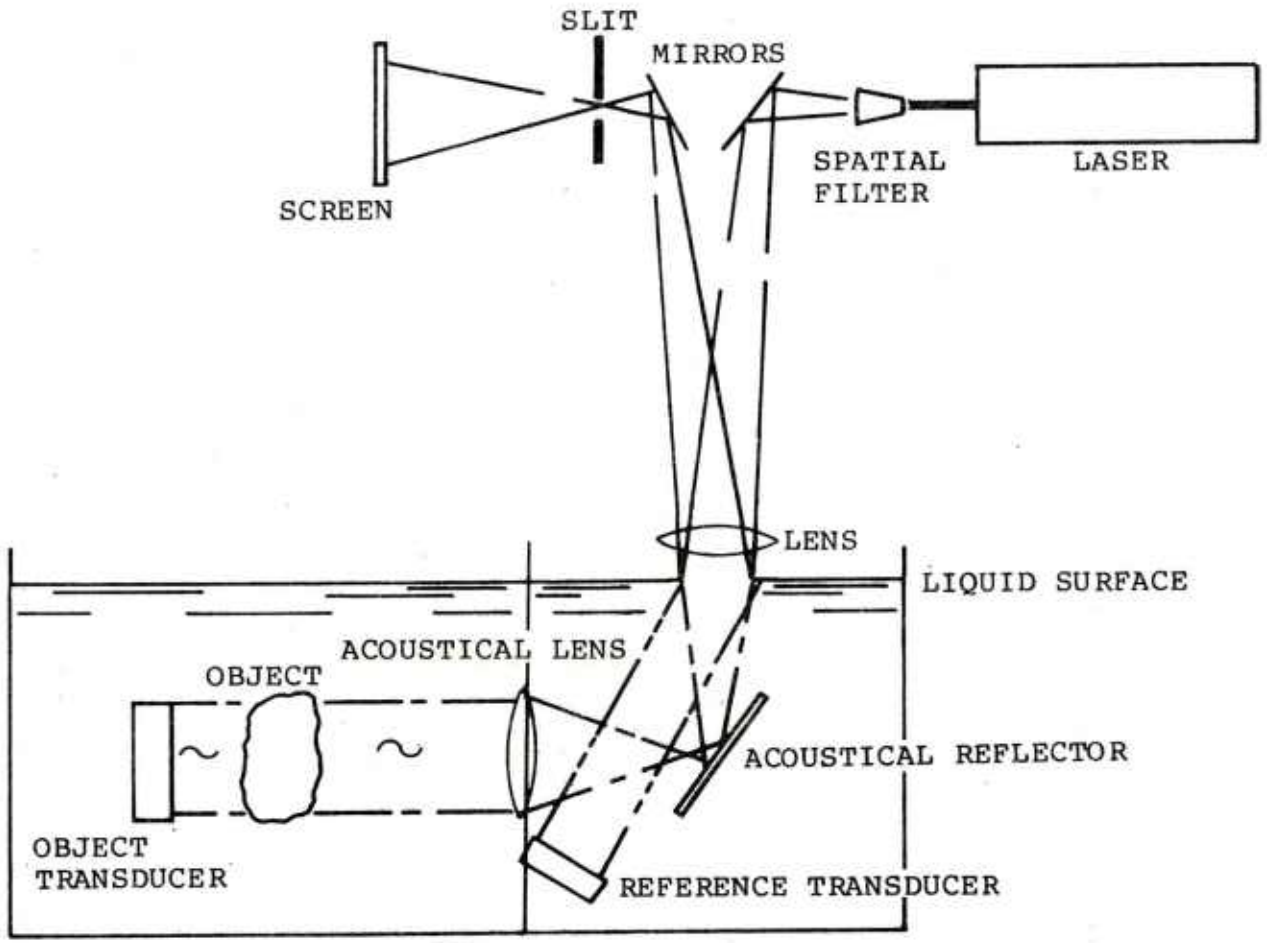

Figure 3. Acoustical holography layout.

at the liquid surface. Reference Figure 4, point 1 notes the transfer tank which still effectively isolates the ripple surface from the object motion, point 2 notes the lens holder, point 3 labels the object holder, point 4 labels the object transducer. The system was effectively isolated from unwanted vibration by being mounted on a 3/4" x 4' x 10' piece of plywood which in turn was supported on 12 small inner tubes. Figure 5 shows the plywood being held off the floor by the inner tubes. The inner tubes are 16" diameter and are interconnected with tygon tubing so that all tubes have the same pressure. The pressure in the tubes is about 5 psi, purposely small for a "softer" spring effect to reduce vibrations from the floor to the acoustic system.

Figure 6 is a view of the liquid freon lens which can be adjusted and clamped in place for better alignment.

Figure 7 pictures the reference transducer (point 5) and the object beam reflector (point 6).

Figure 8 illustrates the external object support (point 7) that was rigged from available material at the time, but was effective. A TV monitor and recorder are shown (point 8).

Figure 9 pictures the optical system the laser (point 9), the spatial filter (point 10), mirror housing (point 11), lens housing (point 12), mask (point 13), slit (point 14), ground glass and cover (point 15).

Figure 10 illustrates the electronic controls with Figures 11, 12, 13 showing closer views and with Figure 14 showing the back of the electronic controls.

Figure 15 shows the TV camera location.

C. Turning the System On

Spectra Physics has published a manual for the operation of their laser and a manual for pulsing the laser. These manuals should be referred to for laser operation. Of note is that the acoustical system works as well with the laser in continuous wave (CW) mode as in the pulse mode. Because the intensity is greater in the CW mode this might be the preferred mode. Also 50 milliwatts CW laser power does an excellent job of imaging the ripple surface, thus a helium neon laser could be used.

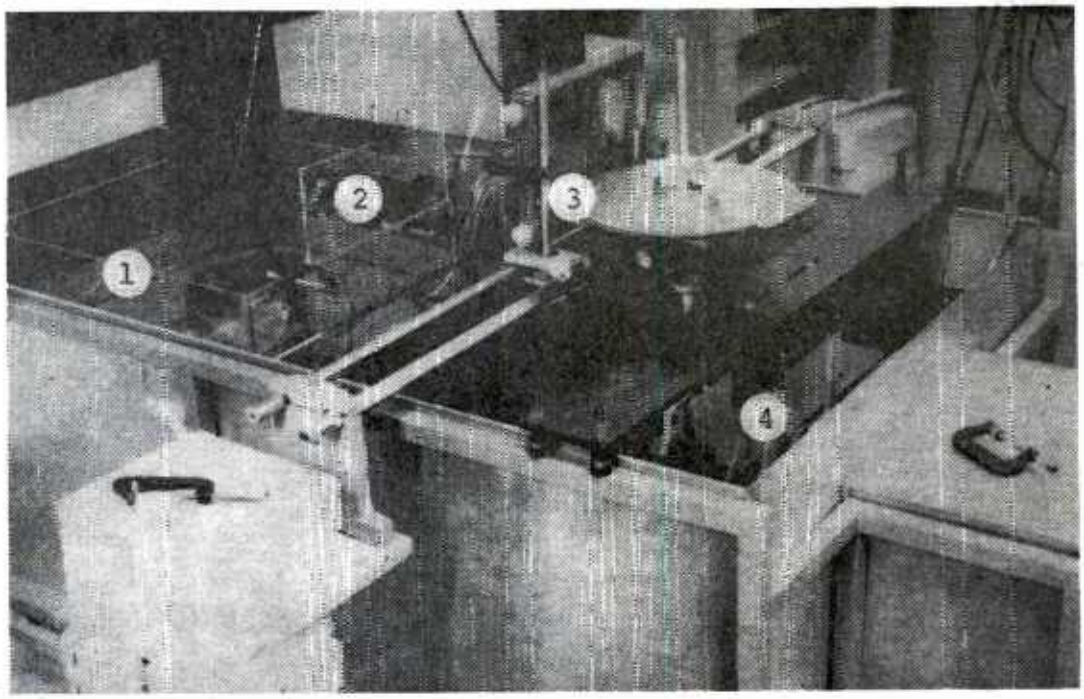

Figure 4. 'ARTHIR' rearrangement.

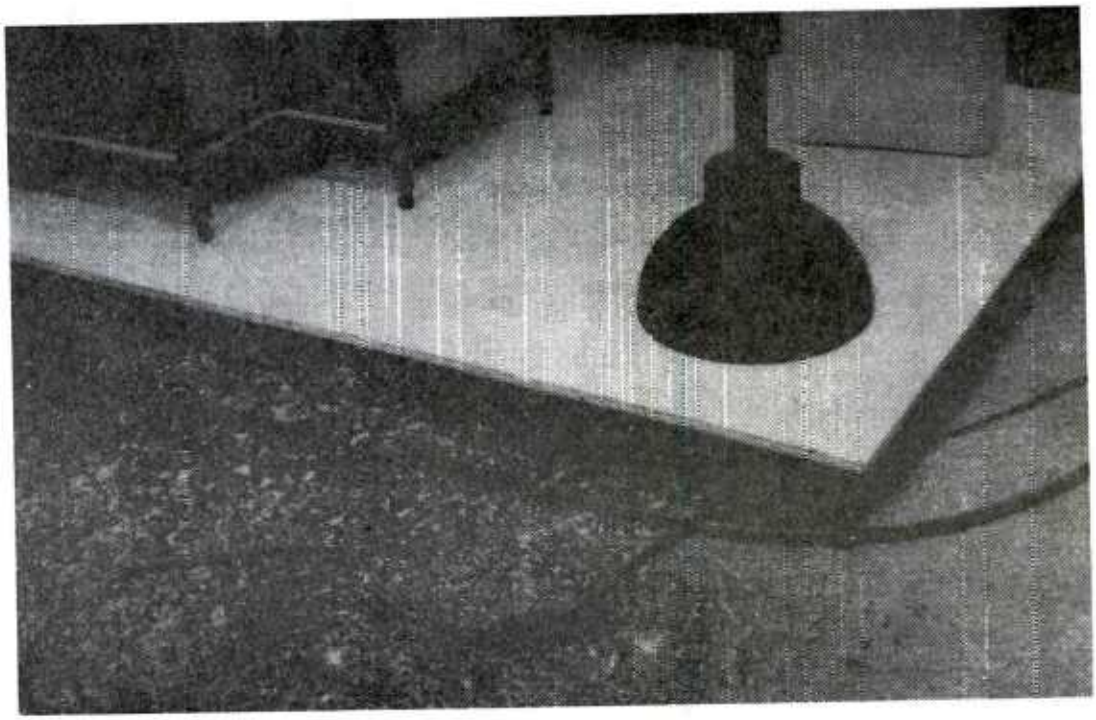

Figure 5. System isolation.

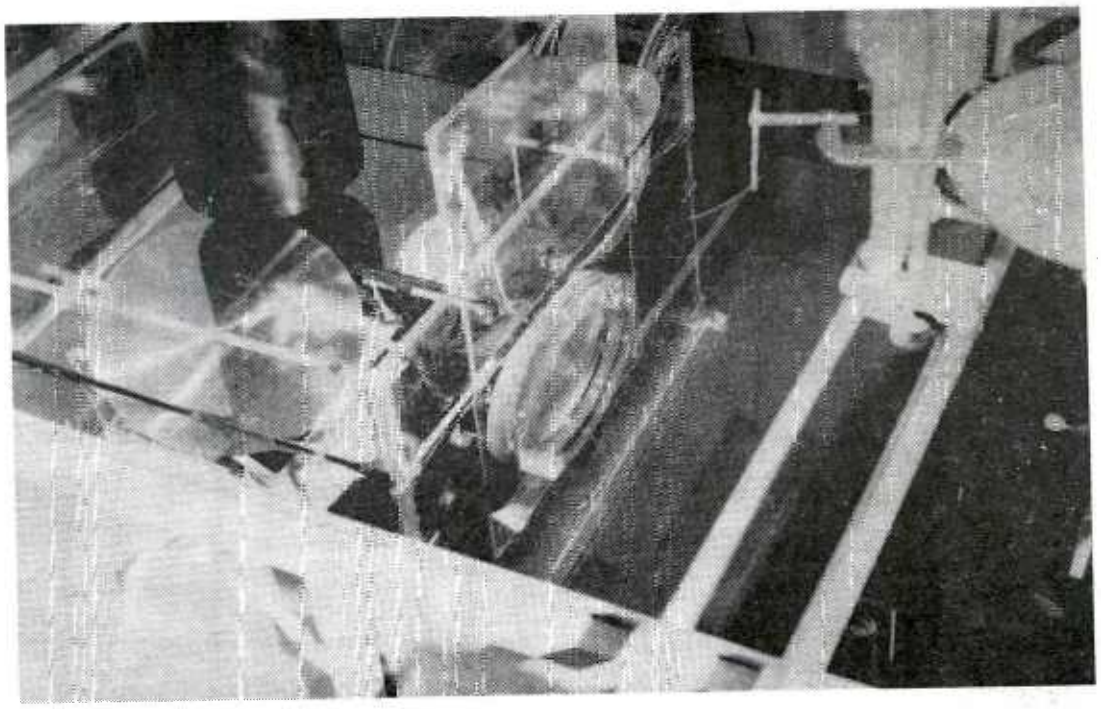

Figure 6. Acoustical liquid lens.

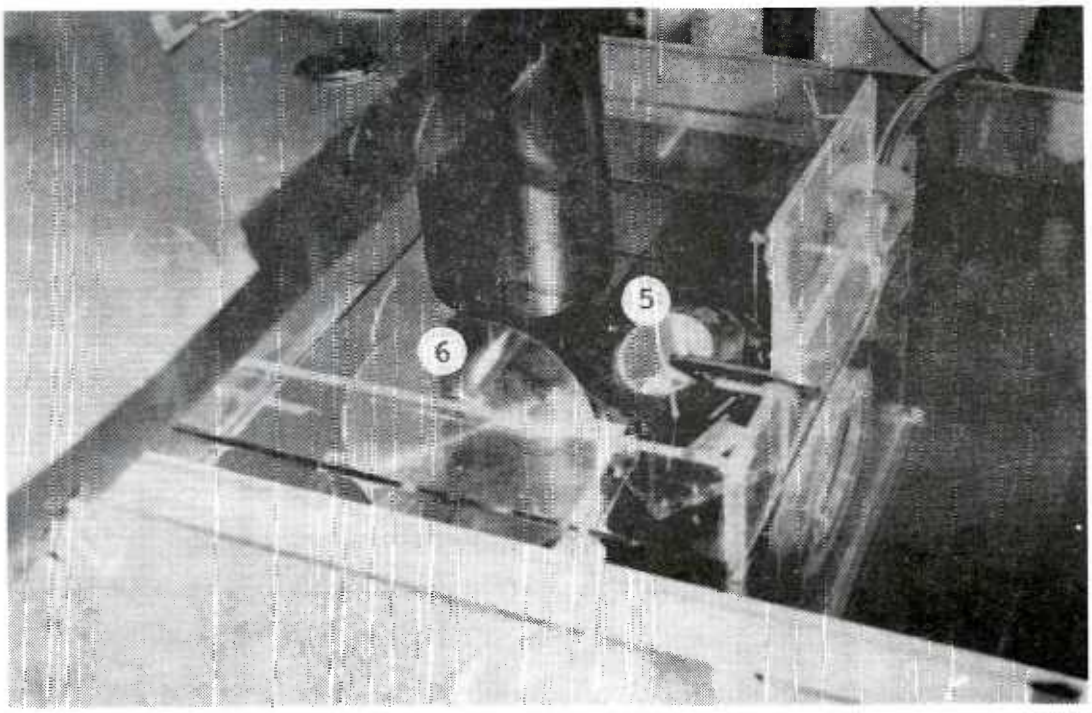

Figure 7. Reference transducer and reflector.

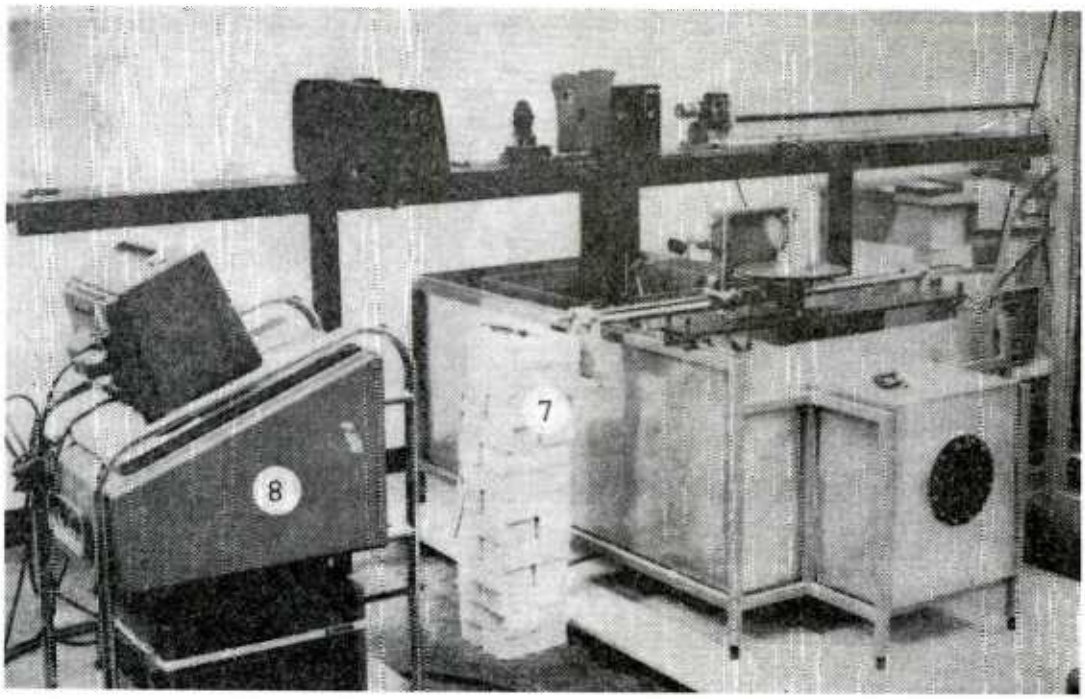

Figure 8. Object support.

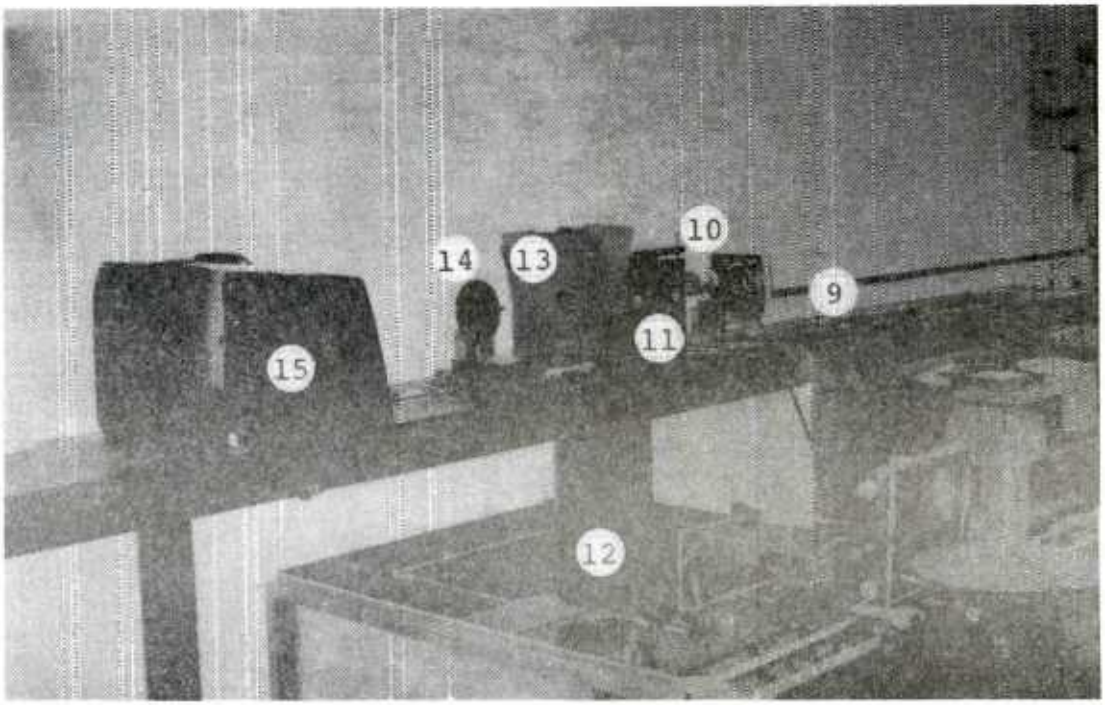

Figure 9. Optics.

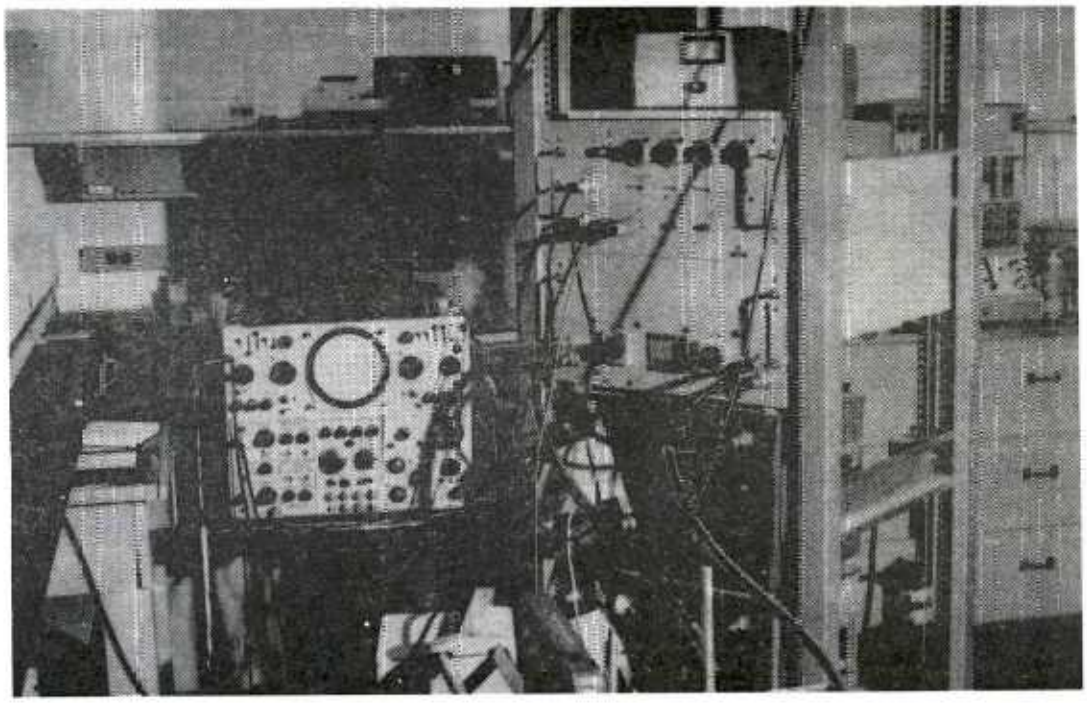

Figure 10. Electronic controls.

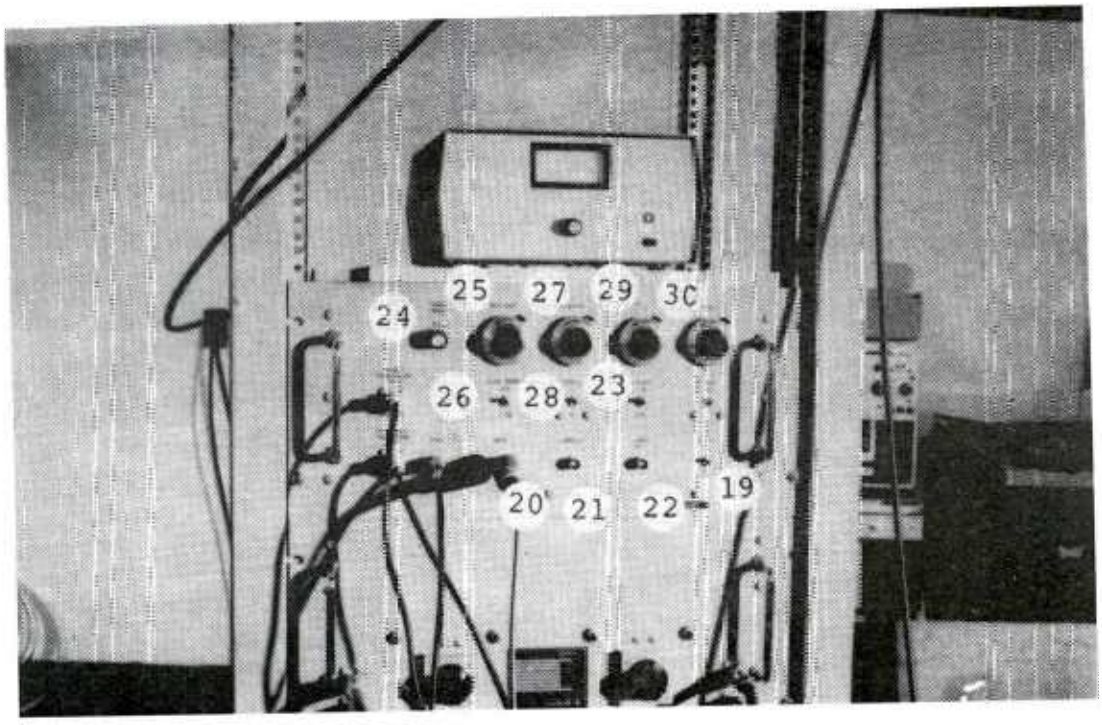

Figure 11. Timing and monitor controls.

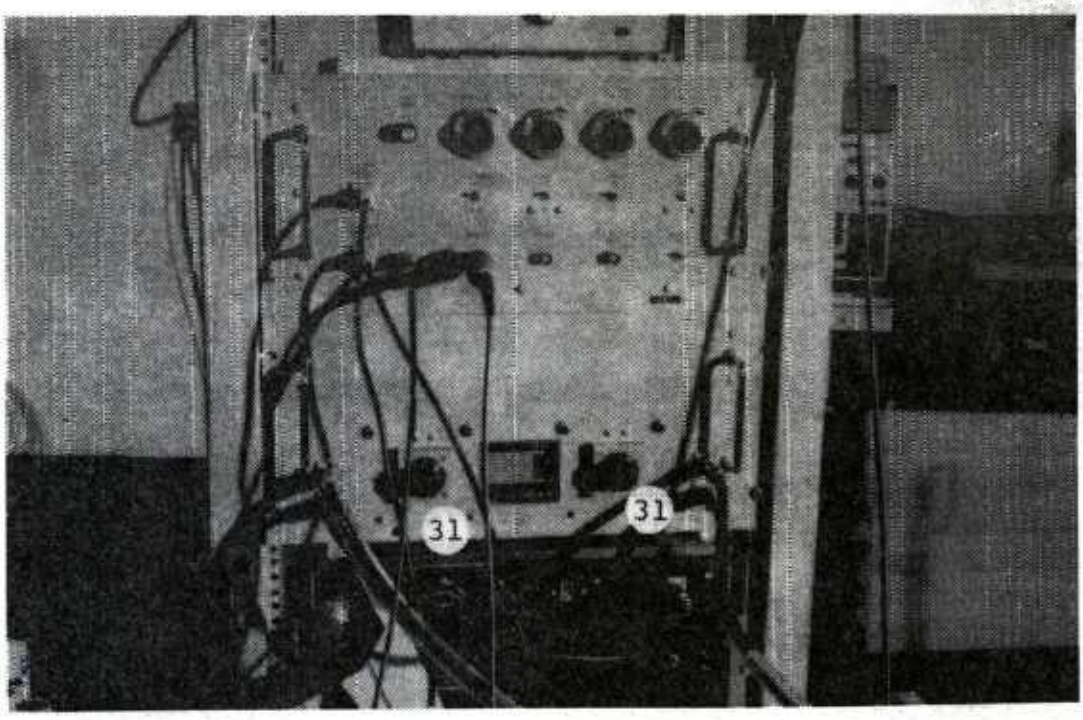

Figure 12. Capacitors.

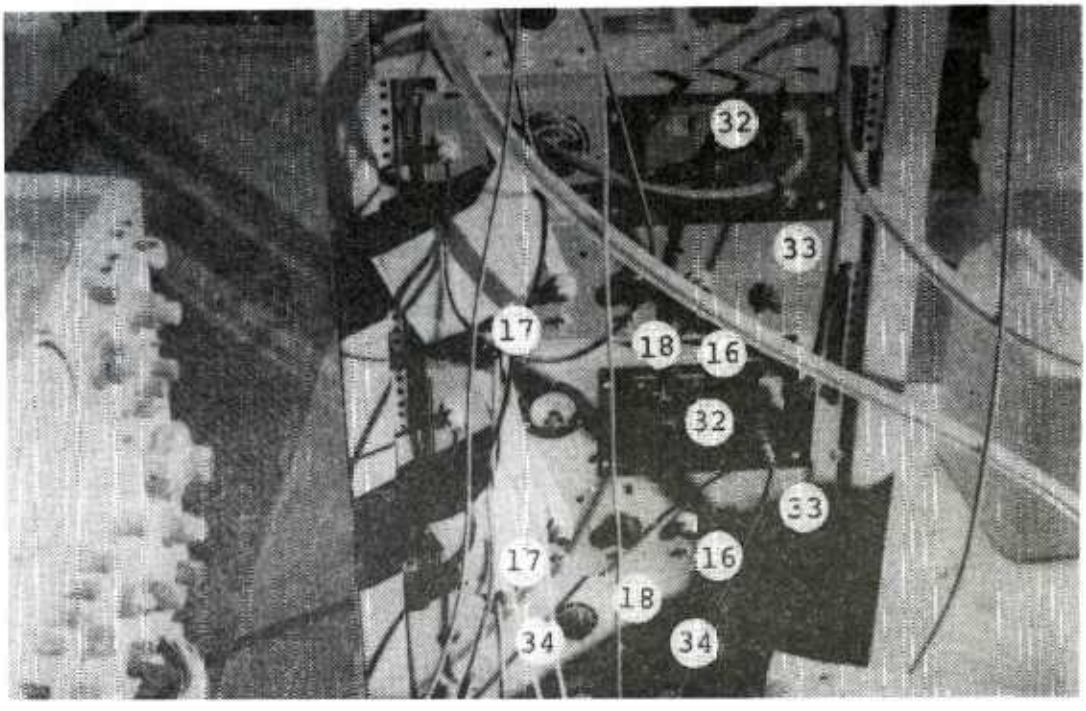

Figure 13. Power supply and controls.

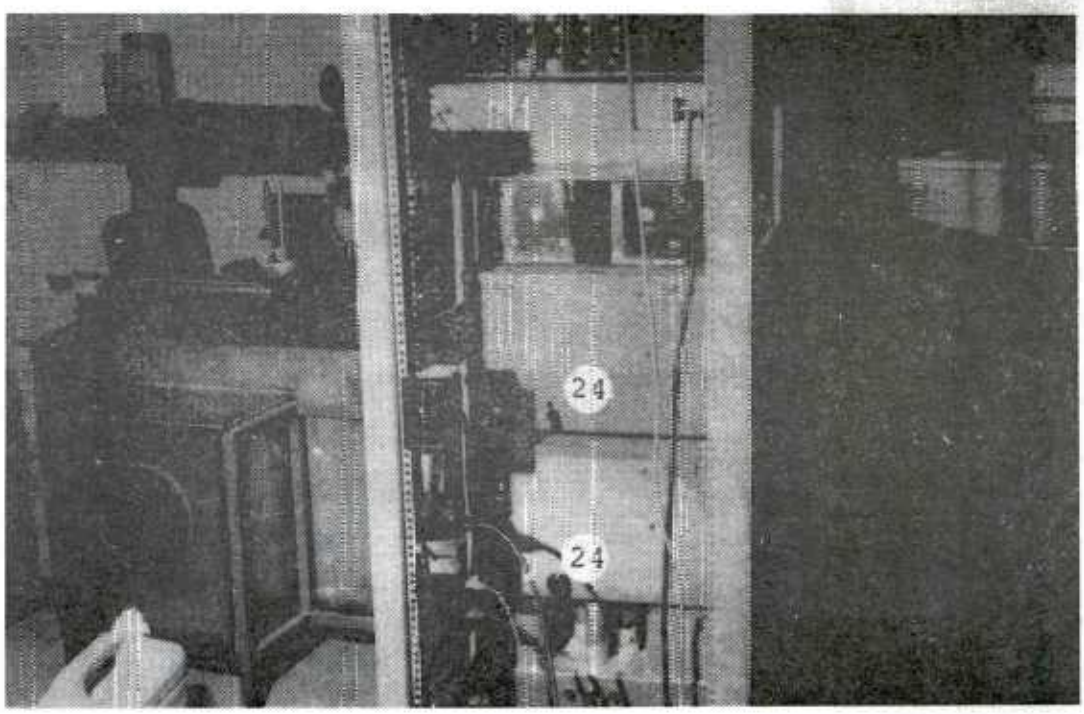

Figure 14. Oscillator controls.

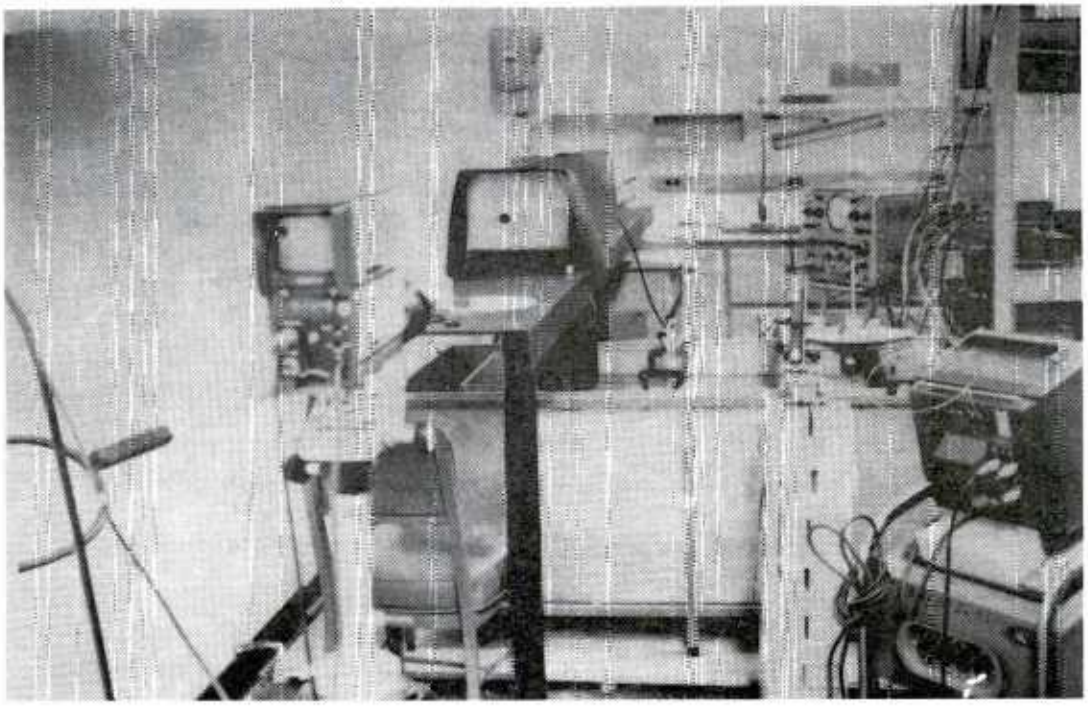

Figure 15. TV Set-up.

A description of the operation of the acoustical system is given by Ireland, Mullinix, and Castle in Technical Report T-78-10 and the reader should reference this work.

A description of the electronic controls is reported by Sperry Rand in Technical Report No. SP-271-0998, "Real-Time Acoustical Holography Nondestructive Test System".

There is a TV tape describing the acoustical system, how to align the system, how to operate the system and examples of its use. The tape is by this investigator.

Some of the items referred to are noted in Table 2 for easy identification.

D. Acoustical Alignment Techniques

After the laser has been put in operation (at full power) and after the transducers have been activated the acoustical components need to be aligned and timing delays set for operation.

Start with the object transducer (3 MHz) at maximum power, the reference transducer off, the acoustical lens out, the light slit out, the repetition rate maximum, the width at 200 microseconds, the laser delay at 300 microseconds. Adjust the location of the object beam ripple pattern as seen on the TV monitor to be centered (Figure 16). Turn the power off of the object transducer and turn the reference transducer to about half power and center the ripple as seen on the TV monitor (Figure 17). Turn the reference transducer off and put the object transducer at maximum power. Insert the liquid lens and adjust until the ripple pattern is centered (Figure 16). With the object transducer still on, turn the reference transducer to half power and adjust the reference delay until obvious interference between object pulses and references pulses are seen on the TV monitor. Turn the reference power off. Put the slit at 0.020 inch opening with slit horizontal at the reflected focal point of the laser output. Adjust the slit up and down until the brightest pattern is seen on the TV monitor, now adjust until a shadow blocks out the bright pattern (the zero order diffraction pattern has been blocked and the first order is passed through). Turn the reference to about one fourth power and put an object in for observation. Now adjust controls for the "best" hologram.

TABLE 2. System Nomenclature

ITEM DESCRIPTION	I.D. NO.	FIGURE NO.
Transfer Tank	1	4
Lens Holder	2	4
Object Holder	3	4
Object Transducer	4	4
Reference Transducer	5	7
Acoustical Deflector	6	7
Object Holder	7	8
TV Monitor and Recorder	8	8
Argon Pulse Laser	9	9
Spatial Filter	10	9
Light Deflectors	11	9
Lens Holder	12	9
Mask	13	9
Slit	14	9
Ground Glass	15	9
Power Amplifier Plate Voltage Switches	16	13
Filament Power Switches	17	13
Tune-Operator Toggle	18	13
Power Switch SNDT 2000 Generator Unit	19	11
Object Pulse Envelope, Gate 1 BNC	20	11
Reference Pulse Envelope, Gate 2 BNC	21	11
Laser Drive Pulse Envelope, Laser Drive BNC	22	11
Laser On-Off Toggle	23	11
Freq (MHz) Selects 1,3,5,7 MHz Freq. Pulse	24	11, 14
Repetition Rate Control	25	11
Syn enable, Variable Repetition Rate or 60 Hz	26	11
Pulse Width Control for Both Reference and Object	27	11
High and Low Pulse Width Range	28	11
Laser Delay After Reference Pulse	29	11
Reference Delay After Object Pulse	30	11
Parallel Variable Capacitors	31	12
Cyclometer Adjustment Knob	32	13
Meter Switch Control	33	13
Transducer Power Control Knobs	34	13

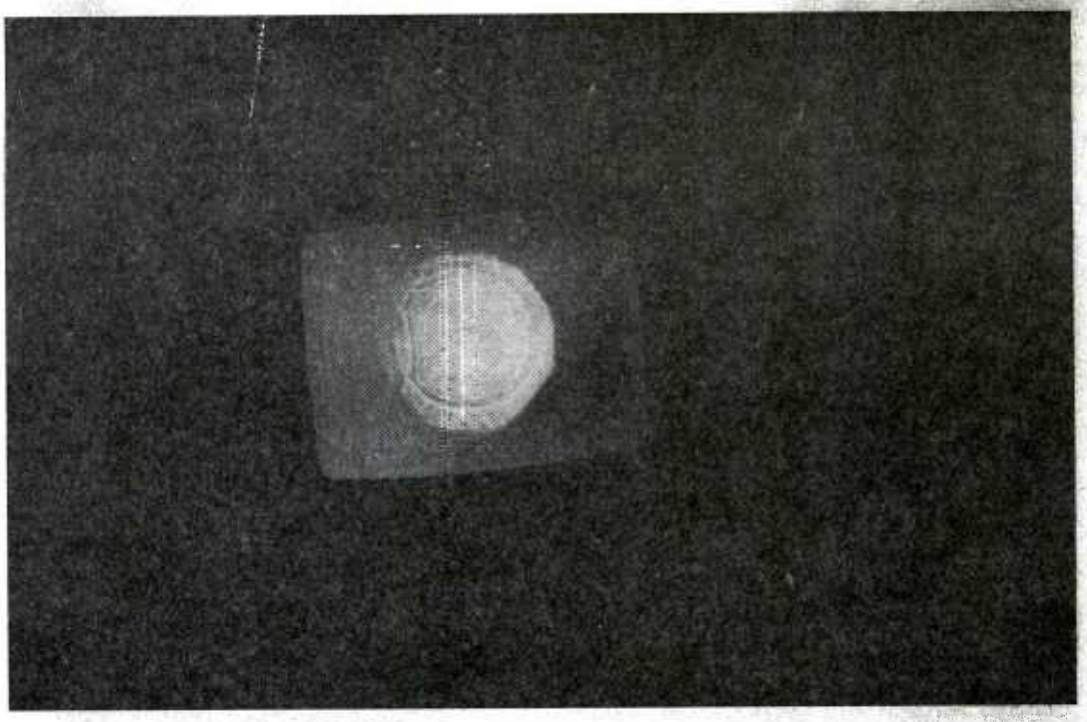

Figure 16. Object beam ripple.

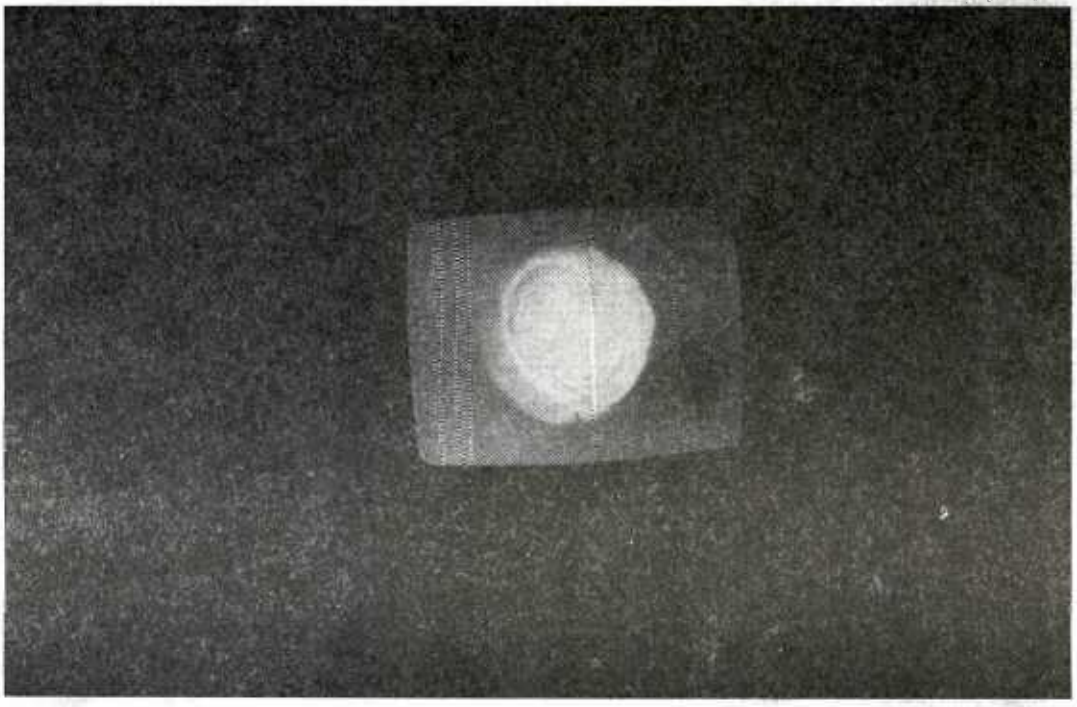

Figure 17. Reference beam ripple.

E. Comments on Components in the System

The electronics seemed to work very well.

In use only the 3 MHz mode was practical. The 1-MHz excitation had too much scatter and gave no reasonable results. The 5 MHz excitation mode gave holograms with the most definition but was limited to thin models for lack of strong sonification at 5 MHz compared to 3 MHz. Compare the hologram definition of a small plexiglass "L" with a bolt in one leg shown in Figure 18 and 19. The image in Figure 18 was made with 5 MHz (repetition rate of 5 milliseconds between repetitions, 74 microsecond pulse width, 790 microsecond laser delay, 450 microsecond reference delay - are representative values). Figure 19 is the same model but at 3 MHz. This image is more transparent but the edge definition is not as good. Note that both pictures were made using a minitank to further isolate the ripple pattern. Figure 20 shows the same model with 3 MHz excitation but without a minitank. The image clarity is improved and it is reasoned that the bottom of the ripple tank (a Mylar film) absorbed part of the acoustical energy. It is recommended to investigate ways to improve the high MHZ outputs. High frequency insonification is preferred if high power levels are possible. Perhaps a transducer crystal tuned for a specific high frequency would be possible. The 7 MHz excitation for this system was very ineffective in that no significant power was realized.

Consider the object tranducer. In most holography systems a far field is preferred for holograms. The reason is because of local interference in the near field. This variation is discussed by Zemanek, Joe, "Beam Behavior Within the Nearfield of a Vibrating Piston," The Journal of the Acoustical Society of America, Volume 49, Number 1 (Part 2), 1971 and one example is reproduced in Figure 21. At axial distance "1" the far field is assumed formed. The author gave three dimensionsal illustrations and one is reproduced in Figure 22. Because of these local variations uniform insonification is not expected and would seemingly affect the resulting holograms. However for the transducers in this system the far field doesn't form until approximately 38 feet for the 3 MHz excitation. Even if it was practical to bounce the acoustical wave around until this length was realized, the attenuation caused by the water would absorb most of the acoustical power. Therefore it seemed practical to accept the nearfield disadvantage

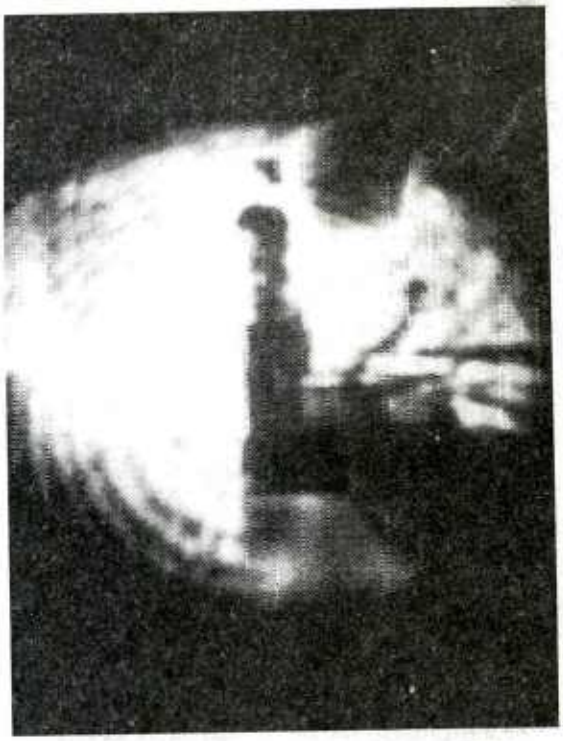

Figure 18. 5 MHz image.

Figure 19. 3 MHz image.

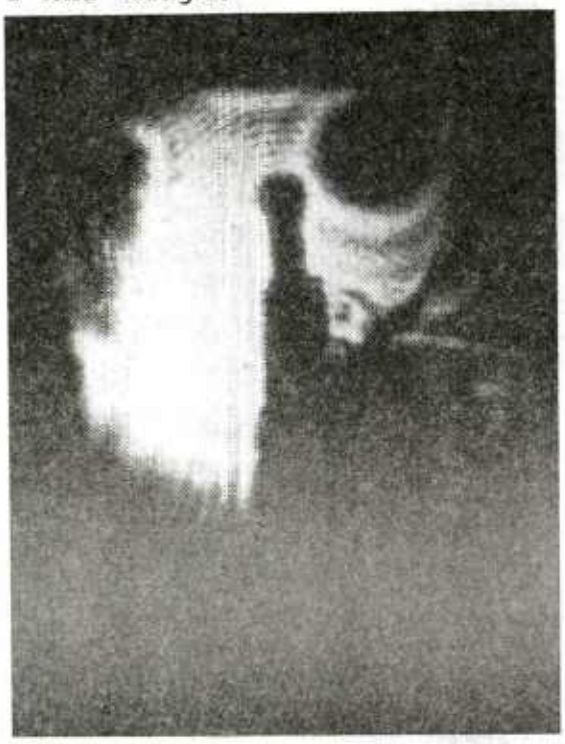

Figure 20. 3 MHz, without minitank image.

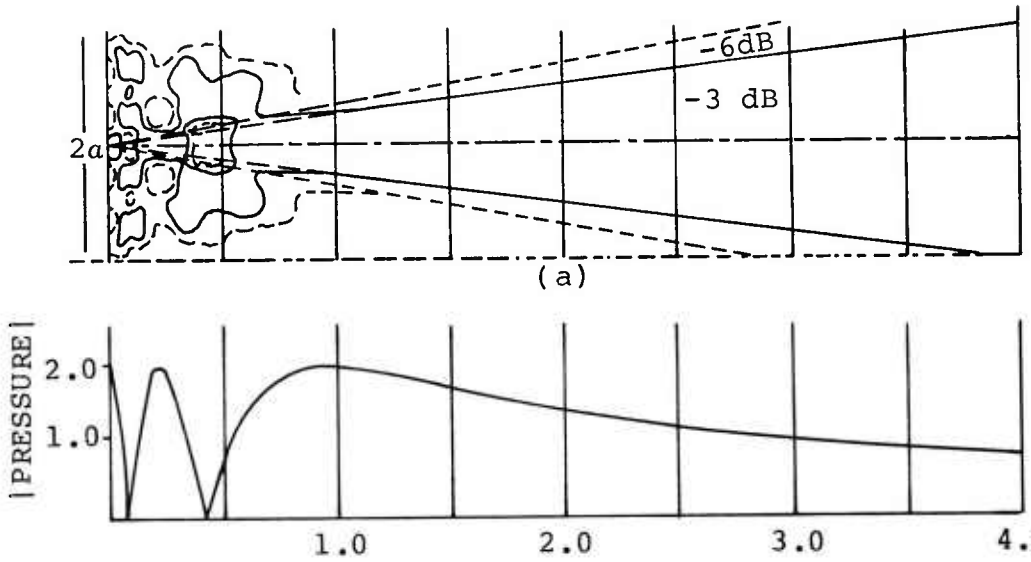

(a) Sound-pressure contour derived from computed data in near- and farfield of circular transducer ($a/\lambda = 2.5$). (b) Magnitude of on-axis pressure variations.

Figure 21. Nearfield pressure versus axial distance.

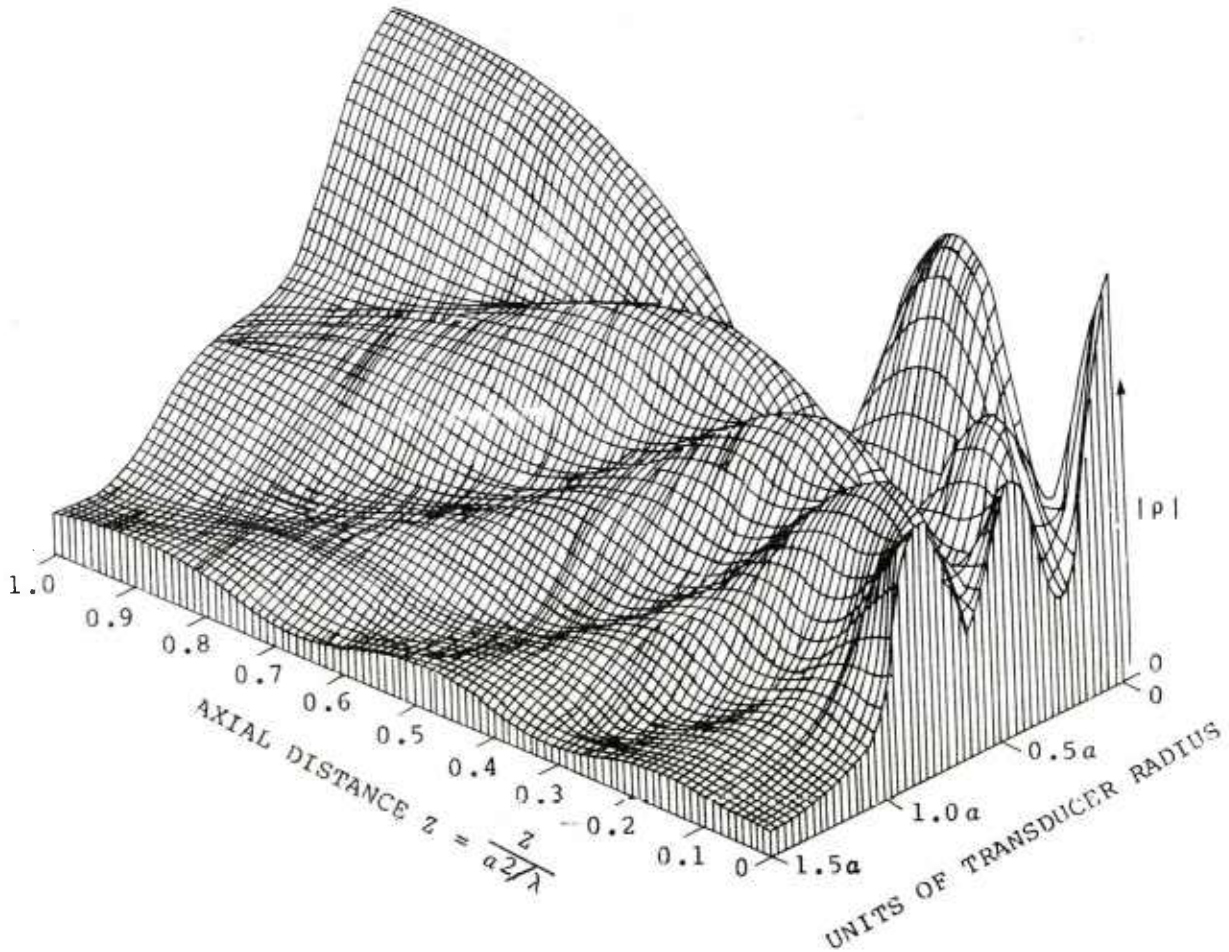

Magnitude of sound pressure computed on grid within nearfield of circular transducer (a/λ=2.5) using exact equation.

Figure 22. Nearfield pressure distribution.

and put the object transducer as close to the object as possible for the extra acoustical power available to the object.

The next element in this system was the acoustical lens. Of the lenses available there were two liquid freon double convex lenses, one glass lens, and one nylon lens available for examination. Also a liquid freon plane convex lens was made. The two liquid freon double convex lenses were contained between Mylar film and are reasonably spherical. The focal lengths were determined experimentally (using holography with image and object distances) to be 6.7 inches and 8.8 inches. These values compared favorably with the values calculated using some "rough" measurements of the lens curvature of 6.6" and 8.0". These lenses seemed to function best in comparison to the other available lenses. The glass lens had a focal length of 20" but did not give as "good" a hologram as the liquid lenses. Probably the extra reflected energy and the production of both transverse and longitudinal waves within the lens account for the decrease in hologram quality. The nylon lens had a focal length of 15" but seemed to absorb considerable energy therefore was not as desirable as the liquid lenses. A liquid freon lens was made and was contained on one side by a plain piece of plexiglass and on the other side by a rubber sheet. The concept was taken from Knollman, Bellin, and Weaver "Variable-focus Liquid-filled Hydroacoustic Lens," The Journal of the Acoustic Society of America, Volumn 49, Number 1 (Part 2) 1971. The idea suggests that instead of moving the object to focus and inspect a point of interest the lens focal length could be varied by changing the amount of fluid in the lens. The lens that was made here in the laboratory absorbed too much acoustical energy. However with the proper selection of material for constructing the lens this appears to be a preferred way of examination and is recommended as an improvement.

For use of a compound lens systems, such as the two liquid, Mylar covered lenses, the necessary equations are noted below (refer to Figure 23),

$$s_2' = \frac{f_2 t(s_1 - f_1) - f_1 s_1}{t(s_1 - f_1) - f_1 s_1 - f_2(s_1 - f_1)} \qquad (20)$$

$$m = - \frac{f_1 s_2'}{t(s_1 - f_1) - f_1 s_1} \qquad (21)$$

where

f_1, f_2 = focal lengths of lenses 1 and 2, respectively

m = magnification.

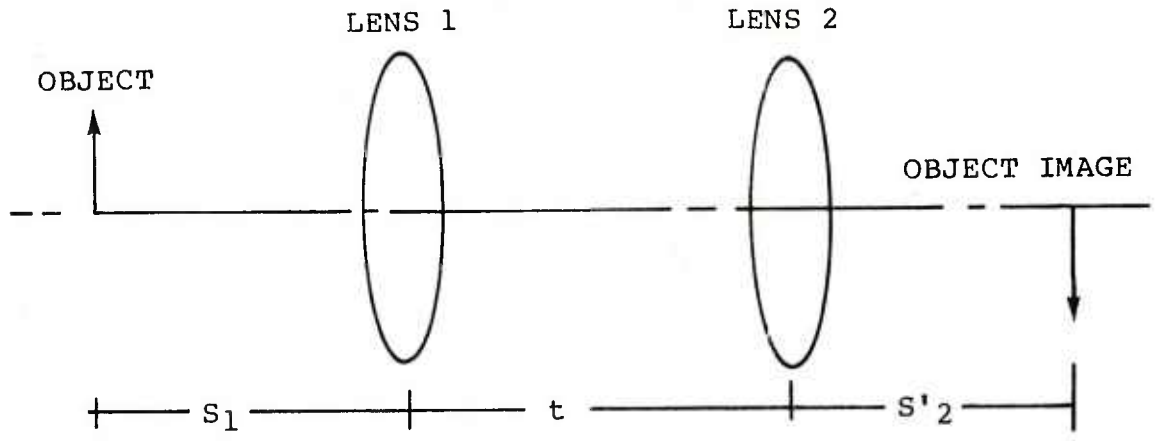

Figure 23. Compound lens system.

Within those two equations there are four variables (m, s_1, s'_2, t). An investigator can select any two and solve for the other two. There are some physical side conditions such as

$$s_1 + s'_2 + t \leq 94" \tag{22}$$

the working distance in the holographic system being described. Examining this side condition, in one case where the object is as far from the object transducer as practical, the object is closer to being in the far field than in any other position; however, this is still not helpful as reasoned out previously. In the second limiting case where the object is as close to the object as possible (meaning $s_1 + s'_2 + t = 94"$) the object is receiving maximum sonification energy. Finally it was found most practical to use only one lens, the alignment was easier, the losses less and the distortion a minimum when compared to a compound lens system.

The next component in the system was the object beam reflector. There was a glass reflector in use and is

satisfactory. A stainless steel reflector was polished and seemed to do better as a reflector than the glass. Theory would suggest that at these angles (45 degrees incident beam) the reflected wave intensity should be the same in glass as in steel (assuming the same surface roughness). For this case the glass probably had a smoother surface and would be expected to give a better reflection. This was not observed. It is recommended that a highly polished steel surface be used as a reflector.

The next component used was a minitank. As noted previously this component's use was discontinued when it appeared that the holograms were more distinct without the minitank than with it (Figure 19 with minitank, Figure 20 without minitank).

The immersion fluid for this acoustical system is water. The possibility of a different immersion fluid should be considered and is recommended. For example glycerin will increase the energy used to insonify a model. In going from water to steel 86 percent of the energy is reflected (14 percent is transmitted). In going from glycerin to steel 78 percent is reflected (22 percent is transmitted). These numbers are for normal incidence. Note that approximately 50 percent more energy is transmitted in going from glycerin to steel compared to going from water to steel. There obviously are other considerations as to whether glycerin would be suitable such as cost and surface tension. The cost could be minimized by using a filtering system to keep particles out of the glycerin. Qualities such as the surface tension are not available for comparison. It is recommended that glycerin be considered as a new immersion fluid for the acoustical system.

Some design of new components is needed:

- An object holder that can be moved in the plane of the liquid surface, that can raise and lower the model and that can rotate the object is recommended. Further the object holder should be free standing and not attached to the isolated acoustical part of the system. This will allow real time inspection of a model without excessive interruptions due to water surface disturbance induced by the moving model.

- A lens holder that can be adjusted in a plane perpendicular to the object beam for proper lens alignment is recommended.

- A plane-convex lens made of plexiglass has the potential of being a better lens. It will have less distortion than liquid lenses being more spherical. The acoustical wave can enter essentially normal to its plane surface. Plexiglass is rather transparent to acoustical waves.

Considering the optical system several things were examined. First the possibility of using a CW laser as opposed to a pulse delayed laser was examined. The flaws pictured in Figures 29 and 30 were with a pulse delayed laser. The flaws pictured in Figure 31 were with a continuous laser. The continuous laser hologram is preferred. Some of this advantage is attributed to taking a picture with a high quality camera directly from the ground glass screen as opposed to taking a picture from the TV monitor. Still the continuous laser compared favorably. Only one mask was used in the system which enabled more use of the active interference region of the reference and object wave. Several techniques of blocking out the zero order object beam were examined. One procedure was to put an acoustical absorber at the focal point of the acoustical lens, but this was not as effective as blocking out the zero order diffraction pattern at the optical focal point. Probably this is mostly attributed to the visual control at the optical focal point. Also several variations of blocking out the zero order optical diffraction pattern to include different wire sizes were examined. The most effective was to use a slit 0.020 inches wide as noted earlier.

F. Examples:

An example of the sort of resolution and possible improvement of this suggested system arrangement is illustrated in Figures 24 and 25. Figure 24 shows a piece of plexiglass with an opaque mask. Slots have been cut into the mask. The slots are approximately 0.1 x 1.5 inches. Figure 25 pictures the acoustical hologram.

Figure 26 pictures a 5 x 5 x 0.7 inch-silica model. The model had been inpacted in five locations. Figure 27 is an acoustical hologram where subsurface damage and cracks are evident. Examination of damage extent by use of acoustics is obviously practical.

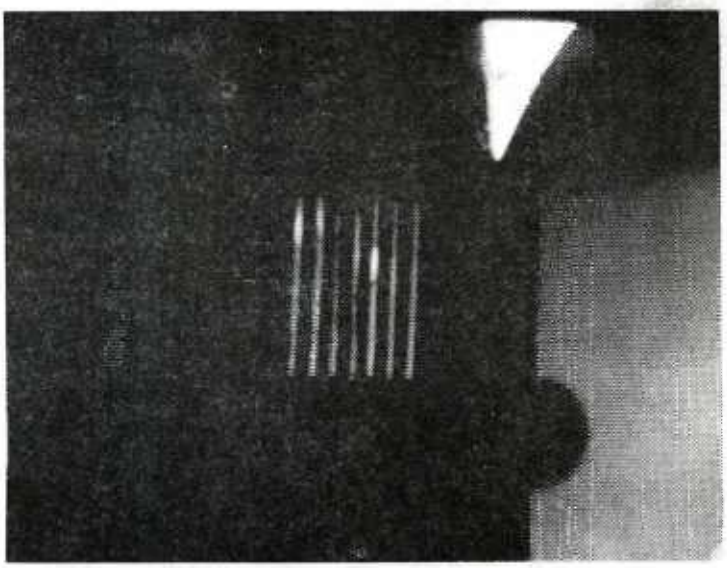

Figure 24. Plexiglass sample with an opaque mask.

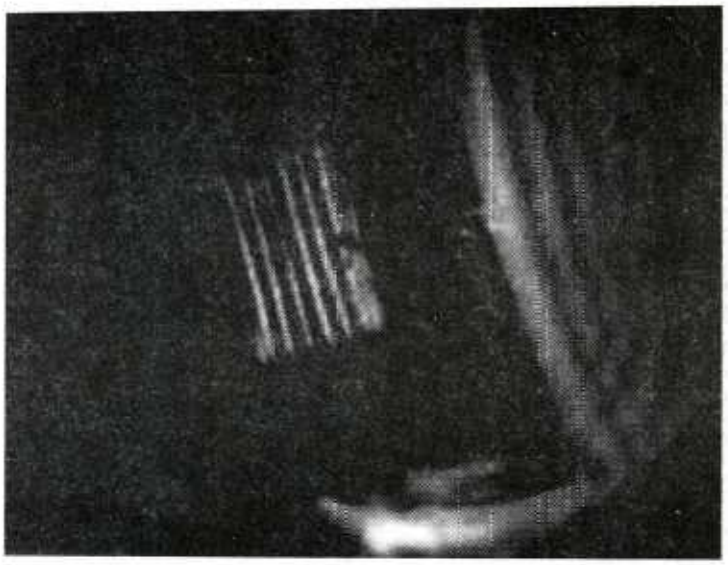

Figure 25. Acoustical hologram of the plexiglass sample with an opaque mask.

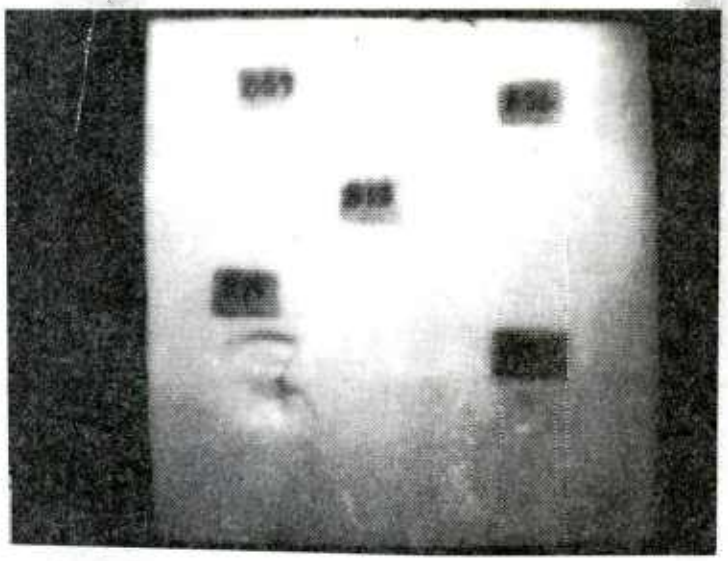

Figure 26. Silica impacted model.

Figure 27. Impacted model hologram.

Figure 28 pictures a 5 x 5 x 0.45 inch-piece of silica bonded to a 0.1 inch piece of stainless steel. The silica side and the steel backing are shown. Two flaws (a 0.5 inch diameter circle and a 0.5 x 1.0 inch-rectangle) were programmed into the bond. Figures 29, 30 and 31 are acoustical holograms of the flaws. Figure 29 and 30 are taken with the laser pulse delayed and are photographs of the TV monitor screen. Figure 31 pictures the flaws and are taken using a continuous laser and photographed on the ground glass screen with a high quality camera. Of interest in taking these holograms is that when the model was precisely perpendicular to the object beam no interior defects could be noted. However, in rotating the model at multiples of half the critical angle the model becomes acoustically transparent and the flaws were very evident. The ability to rotate the model during examination is important. Further, this does demonstrate how disbonds can be detected. The model was examined by insonifying the steel first. Insonifying the silica first was not nearly as effective.

The next example was similar to the model just described. Silica was bonded to steel. A crack (penciled in for helping locate the crack) was in one corner, Figure 32. Also the silica was not constant thickness but tapered from approximately 0.45 to 0.65 inch. The vertical penciled lines shown in Figure 32 are in effect contour lines. Figure 33 shows an acoustical hologram of the crack. The model when rotated showed the crack very well. Also it was noted that vertical bars appeared in the hologram. Figure 34 shows these bars more distinctly as the model was rotated at a larger angle. It is suspected that these are contour line caused by re-reflection of the object beam within the model.

The next example illustrates the ability to detect material separation caused by defects or disbonds with acoustical holography. Figure 35 shows the edge of a 5 x 5 x 0.5 inch-piece of silica bonded to epoxy 0.15 inch thick. Close inspection reveals a vertical crack within the silica and parallel to the epoxy. (There is also a horizontal crack that intersects the exterior surface of the silica and connects to the vertical crack parallel to the epoxy). The crack that parallels the epoxy is about 1.8 inch wide as seen, but extends within the silica 5 inches to the opposite side of the model. Figure 36 shows an acoustical hologram of the model. The dark shadow begins on the right side and the height represents the 1.8 inch dimension of the crack. As the shadow contracts and extends to the

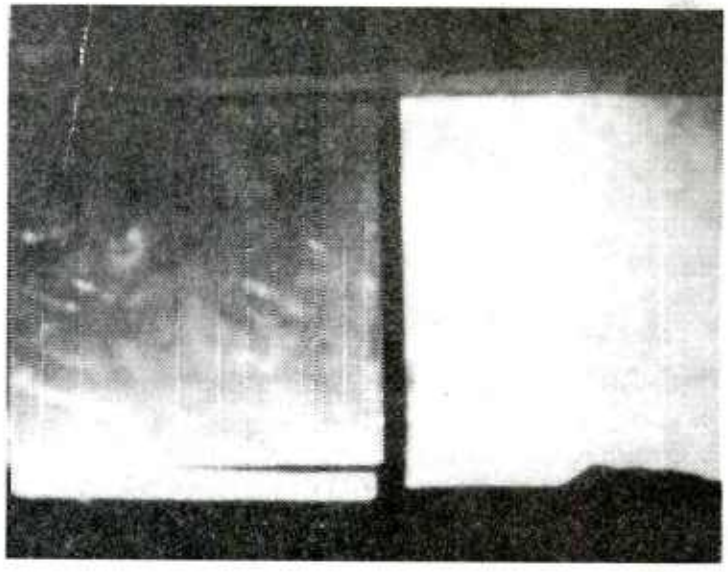

Figure 28. Steel-silica model with flaws.

Figure 29. Circular flaw hologram.

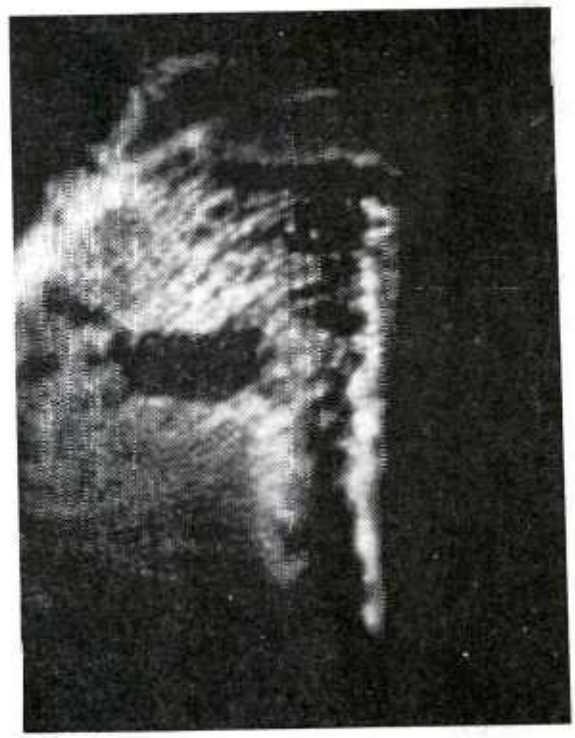

Figure 30. Rectangular flaw hologram.

Figure 31. Flaw hologram with CW laser.

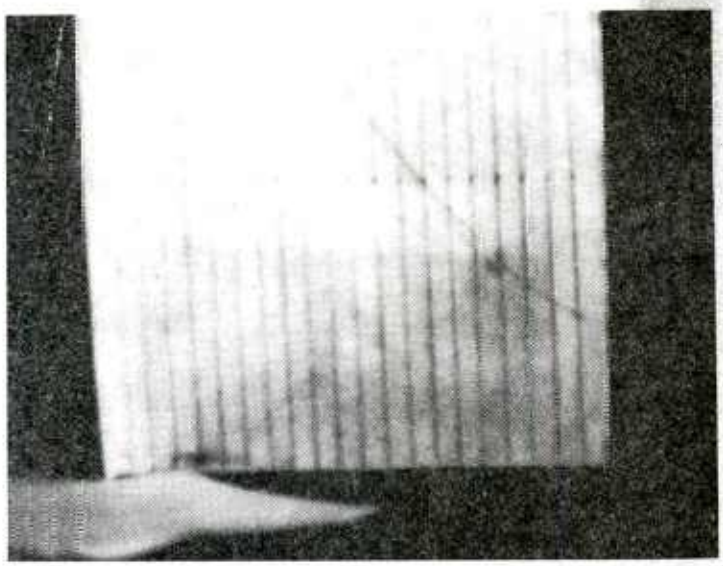

Figure 32. Tapered silica cracked model.

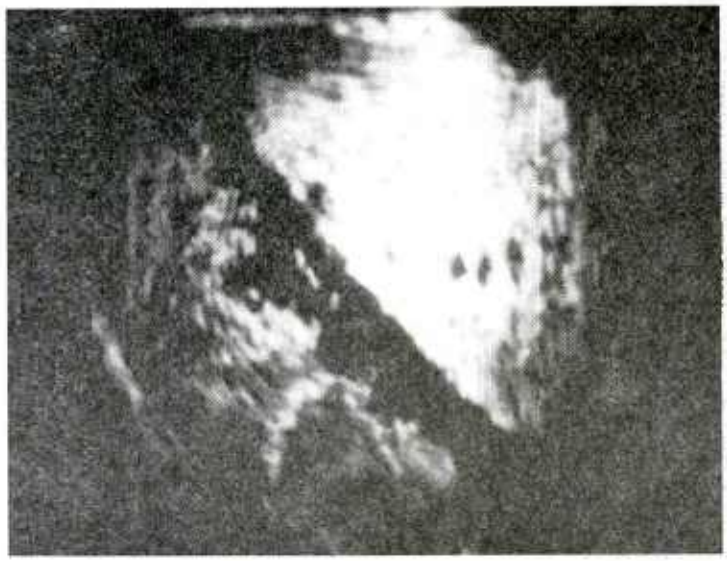

Figure 33. Crack hologram.

Figure 34. Cracks and interference bars.

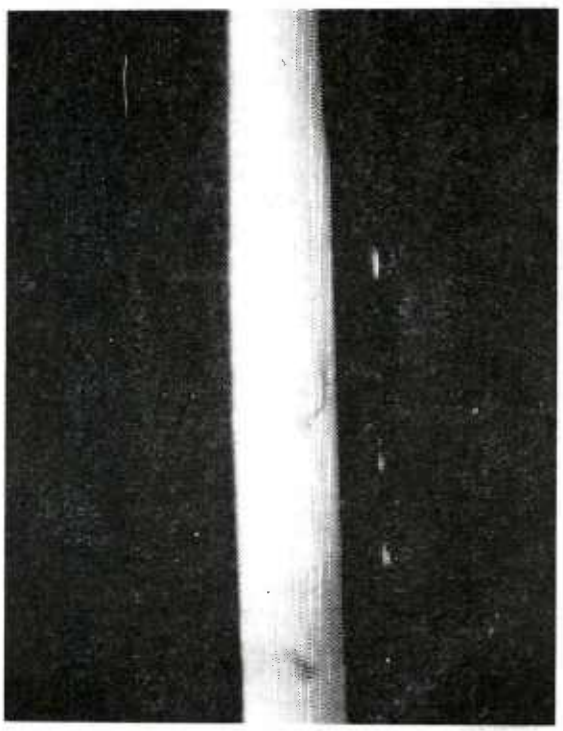

Figure 35. Silica-epoxy internal cracked model.

Figure 36. Internal cracked model hologram.

left, toward the opposite side of the model, the shape of the crack (or disbond within the silica) is noted.

The final example is an epoxy glass thin-walled 3 inch diameter tube, shown in Figure 37. The model has a spot flaw (circle) programmed in the winding of the tube. The spot is a piece of teflon. Figure 38 shows the acoustical hologram of the flaw. The vertical dark bars are characteristics of the cylinder model. The ability to locate disbonds within such fiber glass structures seems evident.

III. Conclusions and Recommendations

The following conclusions and recommendations are given:

1. Examination of solid cylindrical models might be possible with such things as a silica or plaster window (Figure 39) on one or both sides of the model to help collect the acoustical waves.

2. Using the laser in a continuous mode is effective.

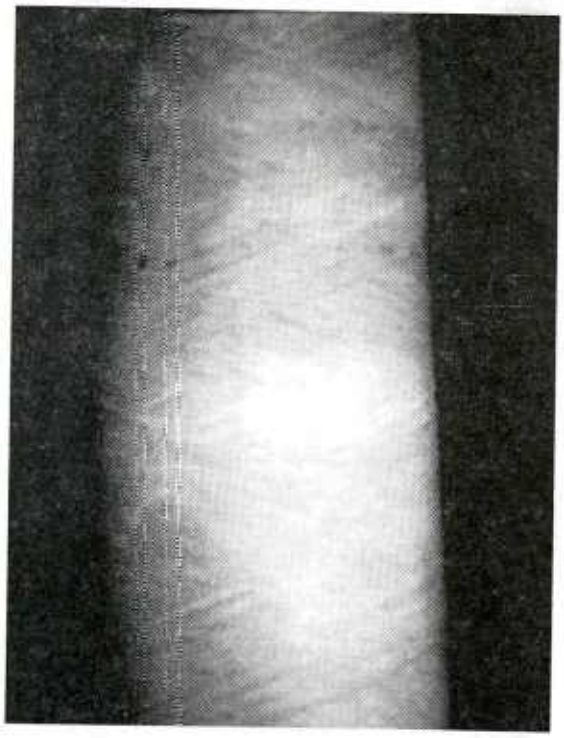

Figure 37. Epoxy-glass cylinder.

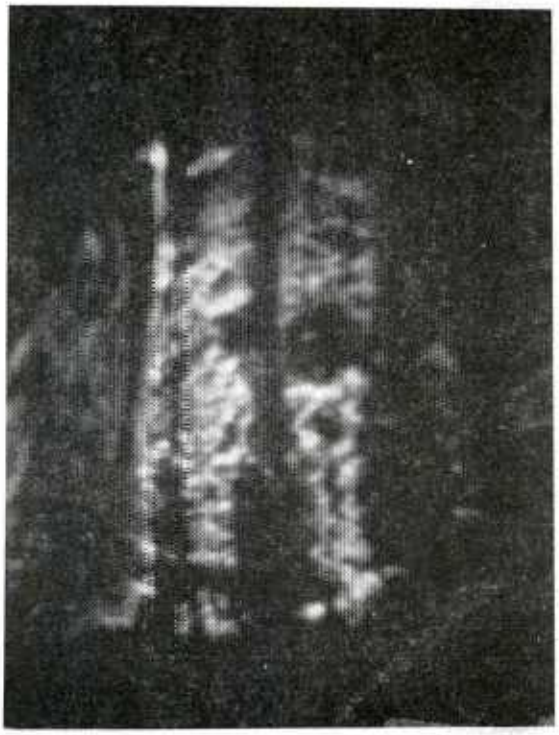

Figure 38. Circular flaw hologram of cylinder.

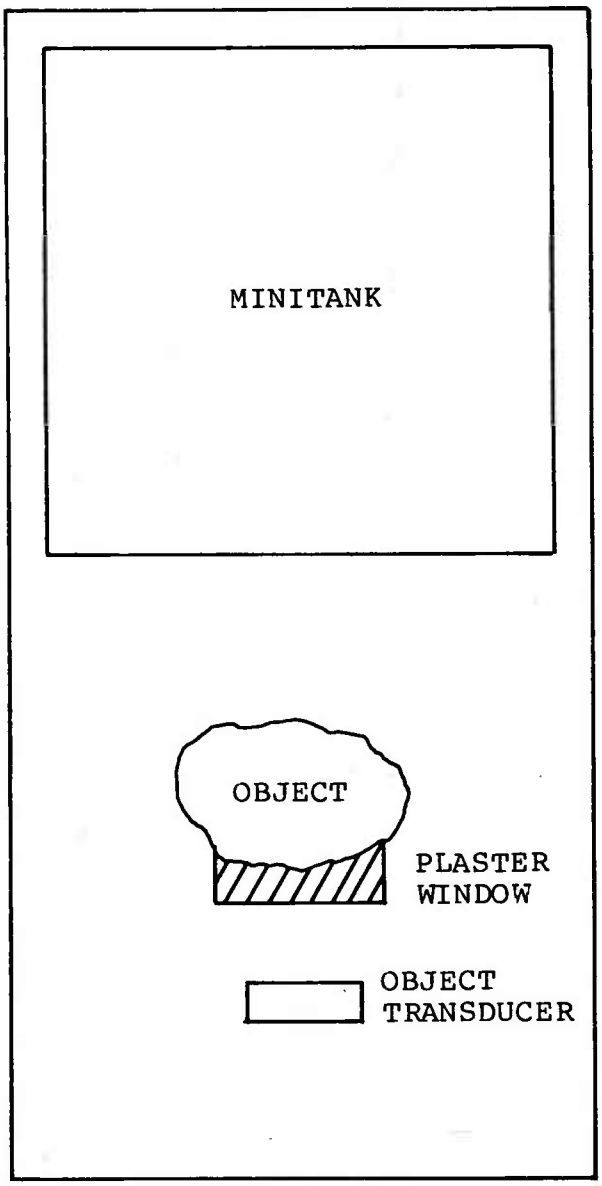

Figure 39. Plaster window.

3. Examine the possibility of having special transducer crystals cut for higher frequency output to give more power for insonifying models.

4. Consider constructing and using a plane-convex plexiglass lens for less distortion.

5. Construct a free standing object support with rotation and three degrees of motion.

6. Construct an acoustical lens holder with two degrees of motion for more precise lens alignment.

7. Consider constructing a plane-convex liquid lens for a variable focal length capability.

8. Consider a highly polished stainless steel reflector for minimum distortion and maximum reflection.

9. Consider using glycerin for the immersion fluid as 50 percent more energy will be transmitted through the model.

10. Consider the possibility of using a digital camera and enhance the images with computer filtering.

DISTRIBUTION

	No. of Copies
Defense Technical Information Center Cameron Station Alexandria, Virginia 22314	12
Defense Metals Information Center Battelle Memorial Institute 505 King Avenue Columbus, Ohio 43201	1
Commander US Army Foreign Science and Technology Center ATTN: DRXST-SD3 220 Seventh Street, NE Charlottesville, Virginia 22901	1
Office of Chief of Research and Development Department of the Army ATTN: DARD-ARS-P Washington, DC 20301	1
Commander US Army Electronics Command ATTN: DRSEL-PA-P -CT-DT -PP, Mr. Sulkolove Fort Monmouth, New Jersey 07703	 1 1 1
Commander US Army Natick Laboratories Kansas Street ATTN: STSNLT-EQR Natick, Massachusetts 01760	1
Commander US Army Mobility Equipment Research and Development Center Fort Belvoir, Virginia 22060	1

DISTRIBUTION (Continued)

	No. of Copies
USA Mobility Equipment Research and Development Center Coating and Chemical Laboratory ATTN: STSFB-CL Aberdeen Proving Ground, Maryland 21005	1
Commander Edgewood Arsenal ATTN: SAREA-TS-A Aberdeen Proving Ground, Maryland 21010	1
Commander Picatinny Arsenal ATTN: SARPA-TS-S, Mr. M. Costello Dover, New Jersey 07801	1
Commander Rock Island Arsenal Research and Development ATTN: 9320 Rock Island, Illinois 61201	1
Commander Watervliet Arsenal Watervliet, New York 12189	1
Commander US Army Aviation Systems Command ATTN: DRSAV-EE -MT, Mr. Vollmer St. Louis, Missouri 63166	1 1
Commander US Army Aeronautical Depot Maintenance Center (Mail Stop) Corpus Christi, Texas 78403	1
Commander UA Army Test and Evaluation Command ATTN: DRSTE-RA Aberdeen Proving Ground, Maryland 21005	1

DISTRIBUTION (Continued)

	No. of Copies
Commander ATTN: STEAP-MT Aberdeen Proving Ground, Maryland 21005	1
Chief Bureau of Naval Weapons Department of the Navy Washington, DC 20390	1
Chief Bureau of Ships Department of the Navy Washington, DC 20315	1
Naval Research Laboratory ATTN: Dr. M.M. Krafft Code 8430 Washington, DC 20375	1
Commander Wright Air Development Division ATTN: ASRC Wright-Patterson AFB, Ohio 45433	1
Director Air Force Materiel Laboratory ATTN: AFML-DO-Library Wright-Patterson AFB, Ohio 45433	1
Director Army Materials and Mechanics Research Center ATTN: DRXMR-PL -MT, Mr. Farrow Watertown, Massachusetts 02172	1 1
Commander White Sands Missile Range ATTN: STEWS-AD-L White Sands Missile Range, New Mexico 88002	1
Deputy Commander US Army Nuclear Agency ATTN: MONA-ZB Fort Bliss, Texas 79916	1

	No. of Copies
Jet Propulsion Laboratory California Institute of Technology ATTN: Library/Acquisitions 111-113 4800 Oak Grove Drive Pasadena, California 91103	1
Sandia Laboratories ATTN: Library P.O. Box 969 Livermore, California 94550	1
Commander US Army Air Defense School ATTN: ATSA-CD-MM Fort Bliss, Texas 79916	1
Technical Library Naval Ordnance Station Indian Head, Maryland 20640	1
Commander US Army Materiel Development and Readiness Command ATTN: DRCMT Washington, DC 20315	1
Headquarters SAC/NRI (Stinfo Library) Offutt Air Force Base, Nebraska 68113	1
Commander Rock Island Arsenal ATTN: SARRI-KLPL-Technical Library Rock Island, Illinois 61201	1
Commander (Code 233) Naval Weapons Center ATTN: Library Division China Lake, California 93555	1
Department of the Army US Army Research Office ATTN: Information Processing Office P.O. Box 12211 Research Triangle Park, North Carolina 27709	1

DISTRIBUTION (Continued)

	No. of Copies
ADTC (DLDSL) Eglin Air Force Base, Florida 32542	1
University of California Los Alamos Scientific Laboratory ATTN: Reports Library P.O. Box 1663 Los Alamos, New Mexico 87545	1
Commander US Army Materiel Development and Readiness Command ATTN: DRCRD DRCDL 5001 Eisenhower Avenue Alexandria, Virginia 22333	1 1
Director Defense Advanced Research Projects Agency 1400 Wilson Boulevard Arlington, Virginia 22209	1
Commander US Army Research Office ATTN: DRXRO-PW , Dr. R. Lontz P.O. Box 12211 Research Triangle Park, North Carolina 27709	2
US Army Research and Standardization Group (Europe) ATTN: DRXSN-E-RX, Dr. Alfred K. Nodoluha Box 65 FPO New York 09510	2
Headquarters Department of the Army Office of the DCS for Research Development and Acquisition Room 3A474, The Pentagon ATTN: DAMA-ARZ Washington, DC 20310	2
US Army Materiel Systems Analysis Activity ATTN: DRXSY-MP Aberdeen Proving Ground, Maryland 21005	1

DISTRIBUTION (Concluded)

	No. of Copies
IIT Research Institute ATTN: GACIAC 10 West 35th Street Chicago, Illinois 60616	1
DRSMI-LP, Mr. Voigt	1
DRSMI-R, Dr. Kobler	1
-RL, Mr. Comus	1
-RLA, Mr. Pettey	1
-RLA, Mr. Schaeffel	50
-EA	2
-EAA	2
-EAS	1
-EAM	1
-EAP	1
-EAB	1
-EAT	3
-ICBB	1
-RPR	3
-RPT (Record Set)	1
-RPT (Reference Copy)	1